

# Models and methods for assessing the value of HVDC and MVDC technologies in modern power grids

Annual report

**July 2017**

PNNL<sup>1</sup>: YV Makarov, MA Elizondo, JG O'Brien, Q Huang, H Kirkham, Z. Huang

ORNL<sup>2</sup>: M Chinthavali, S Debnath

MISO<sup>3</sup>: N Mohan, W Hess, D Duebner, D Orser, H Brown, D Osborn

SIEMENS: J Feltes, D Kurthakoti C, W Zhu

---

<sup>1</sup> Pacific Northwest National Laboratory

<sup>2</sup> Oak Ridge National Laboratory

<sup>3</sup> Mid-Continent Independent System Operator

## DISCLAIMER

This report was prepared as an account of work sponsored by an agency of the United States Government. Neither the United States Government nor any agency thereof, nor Battelle Memorial Institute, nor any of their employees, makes **any warranty, express or implied, or assumes any legal liability or responsibility for the accuracy, completeness, or usefulness of any information, apparatus, product, or process disclosed, or represents that its use would not infringe privately owned rights.** Reference herein to any specific commercial product, process, or service by trade name, trademark, manufacturer, or otherwise does not necessarily constitute or imply its endorsement, recommendation, or favoring by the United States Government or any agency thereof, or Battelle Memorial Institute. The views and opinions of authors expressed herein do not necessarily state or reflect those of the United States Government or any agency thereof.

PACIFIC NORTHWEST NATIONAL LABORATORY  
*operated by*  
BATTELLE  
*for the*  
UNITED STATES DEPARTMENT OF ENERGY  
*under Contract DE-AC05-76RL01830*

Printed in the United States of America

Available to DOE and DOE contractors from the  
Office of Scientific and Technical Information,  
P.O. Box 62, Oak Ridge, TN 37831-0062;  
ph: (865) 576-8401  
fax: (865) 576-5728  
email: [reports@adonis.osti.gov](mailto:reports@adonis.osti.gov)

Available to the public from the National Technical Information Service  
5301 Shawnee Rd., Alexandria, VA 22312  
ph: (800) 553-NTIS (6847)  
email: [orders@ntis.gov](mailto:orders@ntis.gov) <<http://www.ntis.gov/about/form.aspx>>  
Online ordering: <http://www.ntis.gov>



This document was printed on recycled paper.

(8/2010)

# **Models and methods for assessing the value of HVDC and MVDC technologies in modern power grids**

Annual Report

PNNL<sup>1</sup>: YV Makarov, MA Elizondo, JG O'Brien, Q Huang, H Kirkham,  
Z Huang

ORNL<sup>2</sup>: M Chinthavali, S Debnath

MISO<sup>3</sup>: N Mohan, W Hess, D Duebner, D Orser, H Brown, D Osborn

SIEMENS: J Feltes, D Kurthakoti C, W Zhu

July 2017

---

<sup>1</sup> Pacific Northwest National Laboratory

<sup>2</sup> Oak Ridge National Laboratory

<sup>3</sup> Mid-Continent Independent System Operator



## Abstract

This report reflects the results of U.S. Department of Energy's (DOE) Grid Modernization project 0074 "Models and methods for assessing the value of HVDC [high-voltage direct current] and MTDC [multi-terminal direct current] technologies in modern power grids." The work was done by the Pacific Northwest National Laboratory (PNNL) and Oak Ridge National Laboratory (ORNL) in cooperation with Mid-Continent Independent System Operator (MISO) and Siemens. The main motivation of this study was to show the benefit of using direct current (DC) systems larger than those in existence today as they overlap with the alternating current (AC) systems. Proper use of their flexibility in terms of active/reactive power control and fast response can provide much-needed services to the grid at the same time as moving large blocks of energy to take advantage of cost diversity.

Ultimately, the project's success will enable decision-makers and investors to make well-informed decisions regarding this use of DC systems. This project showed the technical feasibility of HVDC macrogrid for frequency control and congestion relief in addition to bulk power transfers. Industry-established models for commonly used technologies were employed, along with high-fidelity models for recently developed HVDC converter technologies; like the modular multilevel converters (MMCs), and voltage source converters (VSC). New detailed models for General Electric Positive Sequence Load Flow (GE PSLF) and Siemens's Power System Simulator (PSS®E), widely used analysis programs, were for the first time adapted to include at the same time both Western Electricity Coordinating Council (WECC) and Eastern Interconnection (EI), the two largest North American interconnections. The high-fidelity models and their control were developed in detail for MMC system and extended to HVDC systems in point-to-point and in three-node multi-terminal configurations.

Using a continental-level mixed AC-DC grid model, an HVDC macrogrid power flow and transient stability models, the results showed that the HVDC macrogrid relieved congestion and mitigated loop flows in AC networks, and provided up to 24% improvement in frequency responses. These are realistic studies, based on the 2025 heavy summer Western Interconnection (WI) planning model and EI multi-regional modeling working group (MMWG) 2026 summer peak cases.

This work developed high-fidelity models and simulation algorithms to understand the dynamics of MMC systems. The developed models and simulation algorithms are up to 25 times faster than the existing algorithms. Control algorithms for high-fidelity models were designed and tested for point-to-point and multi-terminal configurations. The multi-terminal configuration was tested connecting simplified models of EI, WI, and Electric Reliability Council of Texas (ERCOT). The developed models showed up to 45% improvement in frequency response with the connection of all the three asynchronous interconnections in the United States using fast and advanced DC technologies like the multi-terminal MMC-DC system.

Future work will look into developing high-fidelity models of other advanced DC technologies, combining high-fidelity models with the continental-level model, incorporating additional services. More scenarios involving HVDC and MTDC will be evaluated.



## Executive Summary

The main motivation of this study was to show the feasibility and benefit of implementing large-scale direct current (DC) systems overlapping the alternating current (AC) power system. The flexibility in terms of active/reactive power control, and the fast response, were viewed as providing much-needed services to the grid, at the same time as economically moving large blocks of energy. Ultimately, the project's success will enable decision-makers and investors to make well-informed decisions regarding the DC systems as an adjunct to the AC grid.

This work, done under the DOE's Grid Modernization Initiative, involved the development and application of models and methods for assessing this combined AC/DC system on a national scale. The multi-objective control and DC system models developed in this project were aimed at current and future issues of regional transmission organizations (RTO), independent system operators (ISO) and utilities. This project built models and ran simulations for realistic future grid scenarios in an AC/DC grid based on estimates of conditions in the summers of 2025 and 2026. Use cases were studied in which DC lines were controlled to support economic values of power transfers, provide ancillary services, prevent instabilities, and reduce losses. This project also concentrates on developing fast and accurate models of DC technologies and exploring scenarios and use cases, such as multi-objective DC control methods and multi-terminal systems.

Two aspects were explored. HVDC systems embedded both within and across AC interconnections were studied. For this, the much-used PSLF and PSS®E computer programs were adapted to model two US interconnections at once. Fast and accurate models of new DC technologies were developed, and scenarios with multi-objective DC control methods were examined.

In particular, the first year of this project focused jointly operating the two largest AC systems in the US, the Eastern Interconnection (EI) and the Western Interconnection (WI). HVDC services as the loop flows and congestion mitigation in a large AC system, and frequency response (inertial + governor response) were examined. It also focused on developing high-fidelity dynamic models of voltage source converters (VSC), the modular multilevel converter (MMC), in point-to-point and multi-terminal configurations.

Our careful selection of the most important topics included frequency response. This parameter characterizes the ability of a system to automatically recover frequency after an event such as generation outage. This is an important reliability system characteristic because it prevents major frequency variations that could lead to a system collapse. System inertia and speed governors installed on generators are part of the response mechanism, and the study added DC control. The present frequency response trend shows a reduction in performance in many parts of the nation's grid. The work of this project showed that the use of DC facilities could provide an artificial frequency response, taking advantage of mutual help between interconnections.

HVDC systems can be used or additionally installed to relieve AC power transfers within service territories. Currently, transfers can be limited by loop flows through neighboring regional system operators, such as ISOs and RTOs. HVDC systems can help to add transfer capacity to the limited AC paths by reducing AC loop flows. HVDC control and operation with a system-wide perspective will increase system utilization and reliability in normal operational contingencies.

The main accomplishments of the first year are shown in Fig S1.

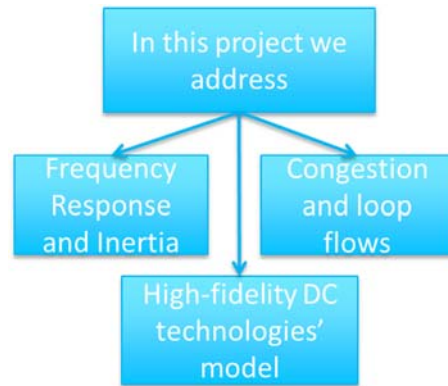


Figure S1. Main tasks in the first year of this project.

## Value proposition

The value proposition of this project includes the following:

- Enable decision-makers and investors to make better-informed decisions regarding the DC systems as an important grid development option. These decisions usually concern major investments and require multiple analyses of the benefits that can be provided. Previously, the analysis does not include the technical and economic benefits of the additional (except the energy transfer) services that HVDC can provide in the combined EI-WI continental-size system. This project has demonstrated that these services become feasible due to the fast response, controllability and flexibility.
- Demonstrate feasibility and reliability of combined AC/DC systems based on existing North American Electric Reliability Corporation (NERC) reliability standards. Increase interest and acceptance of such systems among professional engineers, investors and decision-makers.
- Develop accurate models of DC technologies.
  - Are the existing HVDC models in power system analysis tools, such as PSS®E, adequate for modeling additional HVDC services? The purpose of this analysis is to establish whether the existing HVDC models available in industry-grade power flow and dynamic power systems models are sufficiently accurate to model artificial frequency response. The project team successfully used the example of PSS®E HVDC models, and additionally identified the need in developing of high-fidelity dynamic models of VSCs and multi-terminal HVDC systems for fast-acting applications.
  - What are the opportunities and models for developing publicly-available HVDC models to simulate new technologies and reflect very fast processes, such as electromagnetic transients? The project team has implemented and tested such models and simulation algorithm for accurate dynamic evaluation of voltage source convertor (VSC) types of HVDC systems and new efficient ways for their simulation. Models were developed for point-to-point and multi-terminal configurations.
- Explore multi-objective DC control methods. In particular, this project provides answers to the following important technical questions:

- How to control HVDC systems to achieve this objective? We evaluated two control strategies to implement the frequency response and one strategy to mitigate loop flows and relieve congestion.
  - Can a multi-terminal configuration provide frequency response across different asynchronous interconnections? We developed a multi-terminal VSC HVDC control scheme to show the initial feasibility of connecting to different asynchronous grids (EI, WI, and ERCOT).
  - Examine and compare the local HVDC control strategy (using local signals) vs. the centralized control strategy.
- Develop use cases in which DC lines will be controlled to support healthy values of AC power transfers, provide ancillary services, and prevent instabilities using real-life system models.

## Approach

The approach taken in this project included the following tasks:

- Set up the realistic system Eastern-Western interconnections (EI and WI) models to analyze DC systems embedded within AC large interconnections
- Develop and add macrogrid DC system interconnecting Eastern and Western AC interconnections.
- Develop and test new DC control strategies for multi-objective controls to extract the maximum value from the DC systems in the used realistic use cases (both steady state and dynamic models).
- Test several multi-objective HVDC/MVDC converter control strategies using dynamic power system models that include an interface between the AC and DC systems. Identify the impact on grid reliability and performance. Investigate the impact of HVDC converter control strategies on the DC system.
- Develop AC and DC terminal models of high-voltage DC converters. Implement these models as additions to the Siemens PSS®E simulator.
- Communicate the results to industry partners, the power system community, and decision-makers.

The HVDC model development process includes the following steps:

- Address following challenges in multi-terminal VSC-HVDC systems:
  - Autonomous operation of multi-terminal systems with the ability to provide inertial support to connected AC grids has to be proven, especially with the multi-variable controllers employed in VSC-HVDC (this includes MMC)
- Address features of converter-level control strategies:
  - Hierarchical multiple time-scale multi-variable control algorithms consisting of (refer, Figure S2):

- Estimator: AC-side frequency is estimated based on measured AC-side voltages
- Outer-loop and intermediate control: DC-link voltage, AC-side frequency, and active power are controlled based on expert systems to balance the DC system while responding to AC contingencies like frequency variations
- Inner-loop control: AC currents, DC currents, and internal currents of the MMC are controlled based on proportional and proportional-integral controllers
- Other control loops: Internal capacitor voltages (called submodule (SM) capacitor voltages) of the MMC are balanced and switching actions are taken.

A completed control system might ultimately be configured as indicated in Fig S2.

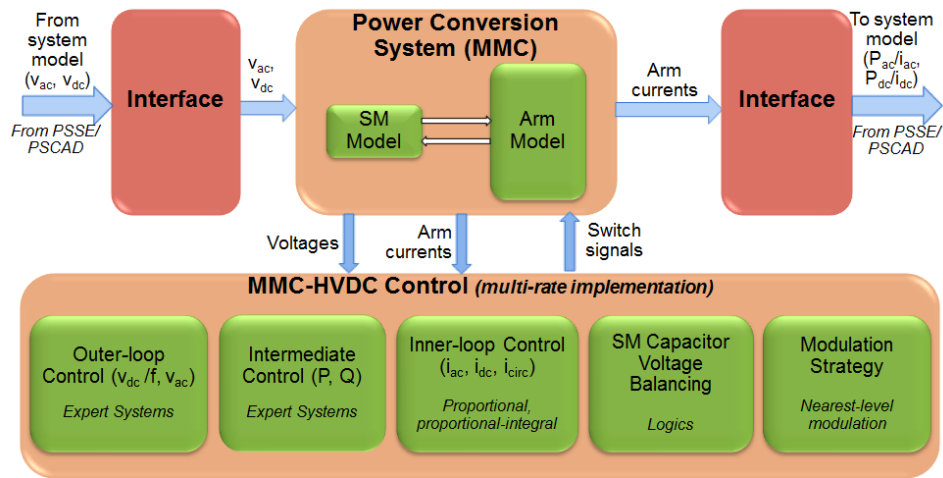


Figure S2. Overview of proposed MMC control strategy for multi-terminal HVDC operation and designed

## Summary of results

### *System models development*

. A first-ever full size nodal AC dynamic model and combined AC-DC model for East and West interconnections was made and demonstrated. The AC systems were interconnected through an HVDC macrogrid, and the case was based on the WECC 2025 heavy-summer planning model and the Eastern Interconnection Multiregional Modeling Working Group (MMWG) 2026 summer peak case.

The team completed a  $\pm 800$  kV point-to-point line-commutated converter-based HVDC Macrogrid across EI and WECC systems, and developed AC power flow models for EI+WI which were N-1 compliant in WI and mostly compliant in EI – see Figure S3.

Besides the use in this project, the new model, as well as the documented model-building procedure, can be used in many other studies looking-ahead into the future grid modernization.



Using the HVDC macrogrid in the EI has several benefits:

- 1) Negate flow in New Madrid transformers (without HVDC it is 13.3% and drops to 1.6% with HVDC);
- 2) Lower impact on highly affected AC lines;
- 3) Selected NERC-defined flowrates have improved.

The potential congestion relief value can be evaluated based on the following considerations:

- Reduce congestion costs: The congestion cost can reach billions of dollars a year, e.g. for New York independent system operator (NY ISO) - \$1.5 billion in 2008; California ISO - \$1 billion for 2004.
- Allow transmission grid to operate closer to the maximum limits.
- Address growing uncertainty, stochastic power flow patterns and loop flows pressing the transmission system's ability to maintain high reliability and continued affordability of power delivery to the limit.

#### *Frequency response modeling and analyses*

In our studies, up to 24% improvement in frequency responses in EI and WI has been demonstrated See Figure S5 and F6.

Two approaches have been developed and successfully tested for HVDC frequency response:

- Autonomous response from each of EI—WI Macrogrid lines.
- Centralized controller approach

Large frequency disturbances were analyzed in WI and EI. For example, the study included a double-Palo-Verde unit outage (~2700 MW), as well as loss of Grand Coulee (~2400 MW), Grand Gulf unit (~1200 MW), and a Fermi unit trip (~1200MW).

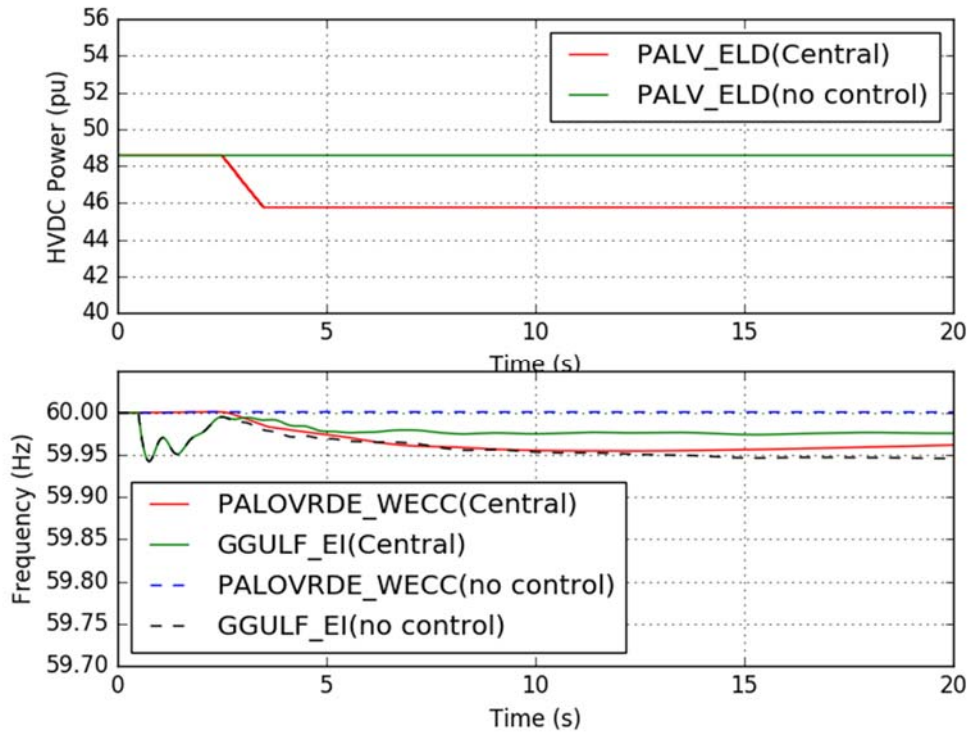


Figure S5. Frequency improvement in the Eastern Interconnection

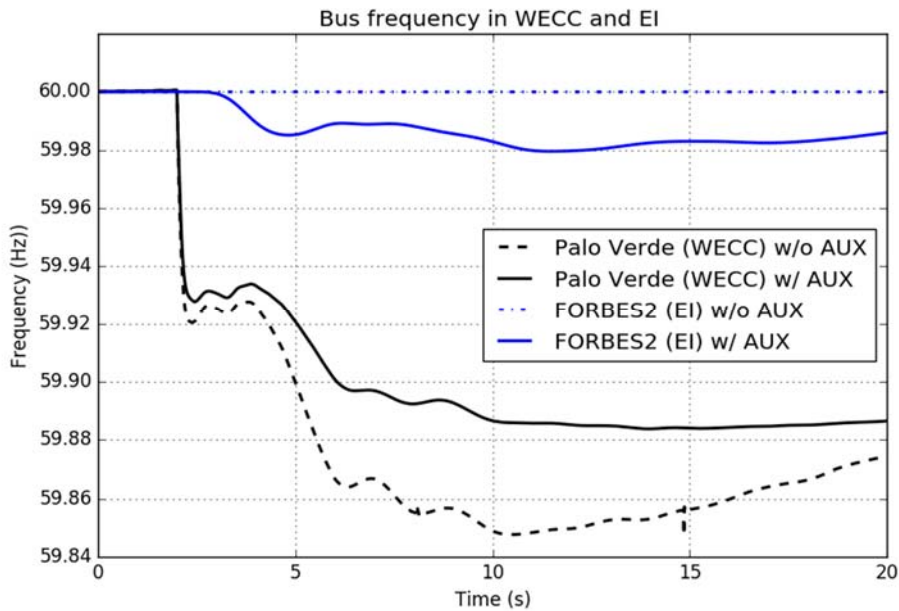


Figure S6. Frequency improvement in the Western interconnection.

The value of frequency response can be characterized as follows:

- (1) Avoid penalties related to frequency response obligation (FRO). The FRO is a NERC standard that requires each entity to provide a sufficient level of frequency response.

- (2) FRO sharing benefits;
- (3) Sharing contingency reserves;
- (4) Prevent load and generation disconnections;
- (5) Prevent cascading outages and blackouts.

An analysis conducted by MISO shows that the frequency response benefits come from:

- \$700,000/MW from capital cost of capacity
- \$13/MWh from frequency response premium.

### Advanced HVDC modeling

Dynamic models and terminal models were developed for MMC VSC using electromagnetic transient (EMT), a program in Fortran90, to interface with large AC and DC system models in PSS®E or Power System Computer Added Design (PSCAD) tools (see Figure S7).

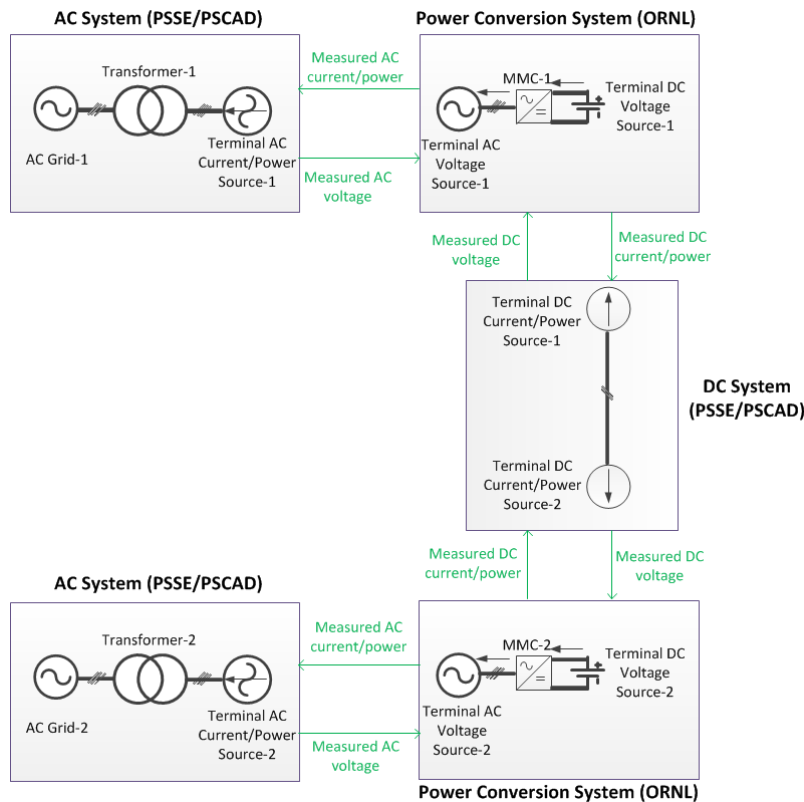


Figure S7. An example two-terminal MMC-HVDC model that has been extended to three-terminals.

Fast dynamic simulation capability observed in the proposed algorithms showed a dramatic improvement in computational speed:

- 200,000 times faster than reference PSCAD/EMTDC models (where EMTDC is an electromagnetic transients and DC algorithms used in PSCAD software)
- Up to 25 times faster than other existing models.

The study was validated with a reference model under following conditions (see Figure S8): steady-state conditions, with changes in power/current, and with DC fault. Errors of less than 1% were found in the models developed.

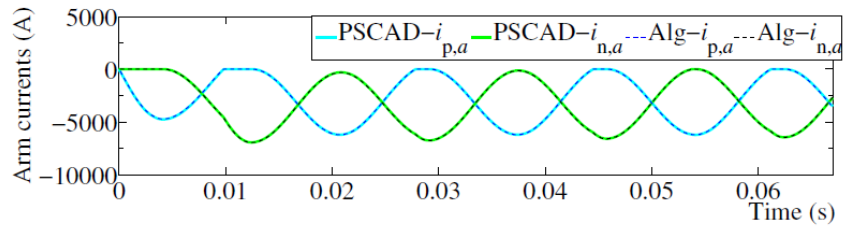


Figure S8. An example of simulation results comparison between developed algorithms (Alg) and reference PSCAD models.

Converter control strategies for frequency response in this new HVDC model were developed and tested as explained below.

A multi-terminal VSC-HVDC model was used to test the frequency response improvements across the EI-ERCOT-WECC simplified model. Aggregated grid models were developed based on NERC frequency response data for each interconnection. A single point of HVDC connection is assumed in each interconnection. Improvements in frequency nadir and settling point post generation loss were found to be between 19 and 45% in each interconnection. Examples are given in Fig S9.

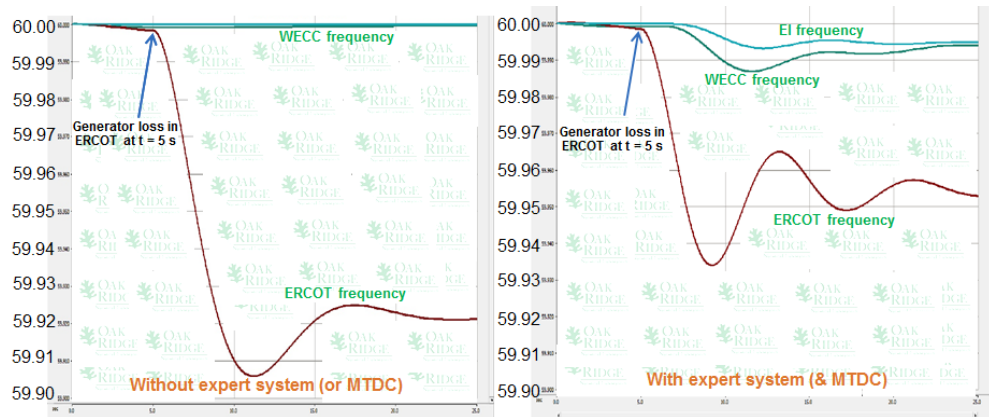


Figure S9. Frequency response to loss of generation in ERCOT: A comparison between case-studies with and without the multi-terminal HVDC.

### Lessons learned and modeling gaps

The major accomplishment is that it has been shown feasible to study the operation of a continental-level interconnected power system employing multiple HVDC lines. The technical feasibility of utilizing industry-grade power flow and dynamic models for combined large US interconnections is now established.

It can now be stated that

- Currently planned infrastructure can accommodate the HVDC injections
- The dynamic performance of the continental system is acceptable
- An HVDC macrogrid can be used to improve dynamic performance by adding auxiliary control to some HVDC lines
- Existing planning tools can be used to conduct this kind of study
- High-fidelity models are required for faster response from VSCs.
- The new multi-terminal VSC simulation approach has been shown to be very successful in terms of accuracy (1%) and performance (200,000 times speed up compared to PSCAD).

Advantages of high-fidelity models for VSC-HVDC:

- Scales to multi-terminal systems.
- It could open the possibility to provides wider range of ancillary benefits like voltage control, black start, islanding.
- Resolves limitations with existing software, by accurately capturing fast dynamics
- Help to avoid long simulation time taken to perform electromagnetic transient dynamic simulation of large AC-DC grids.

### **Proposed future work**

Future work will look into further combining high-fidelity models with the continental-level model. Additional services will be incorporated, and benefits that HVDC and MTDC could provide will be evaluated in more scenarios. It is proposed to

- 1) Develop and evaluate different scenarios of DC system penetrations in the future grid. This work will facilitate understanding of grid expansion plans and the potential benefits, and sensitivities, to scenarios of topology and technology. The multi-terminal DC system models created in first year of this project can be used for this purpose.
- 2) Develop high-fidelity dynamic models of multi-terminal DC systems based on other voltage-source converters (VSCs), such as the cascaded two-level (CTL) converter and alternate-arm converter (AAC). The models developed will enable planners to make better informed choices of the technology in grid expansion plans.
- 3) Build on the three-terminal case-study developed in the first year of this project, studying the feasibility of multi-terminal VSC-DC systems beyond three-terminals. Such a scheme could provide multiple injection nodes in each asynchronous grid. Economic assessments to compare point-to-point LCC systems with multi-terminal systems will be provided.
- 4) Include and rank a greater number of objectives in the multi-objective DC control algorithms. Examples might include strategies to mitigate dynamic contingency response in the DC and AC systems, damping of oscillations, and voltage control. The economic and reliability benefits

associated with such responses and additional services will be studied. Equivalent costs imposed by generation expansion and/or other components to support AC systems will be considered.

- 5) Improve the criteria of selection and placement of the DC technologies based on the aforementioned technical and economic analysis.
- 6) Disseminate findings by organizing industry advisory board meetings and submitting papers to conferences and journals.



## Acknowledgments

The authors would like to acknowledge the support and feedback from Kerry Cheung (U.S. DOE), John Grosh (Grid Modernization Laboratory Consortium (GMLC) Technical Area Lead), H Scribner, E Watson, and J Caspary from the Southwest Power Pool (SPP),

The authors would like to also thank the participants of the Industry Advisory Board: Fred Fletcher (Consultant), Irina Green (California Independent System Operator (CAISO)), Sharma Kolluri (Entergy), Hassan Ghoudjehbklou (San Diego Gas and Electric), James Hirning (Western Area Power Administration), Maryam Saeedifard (Georgia Tech), James Wong (Bonneville Power Administration (BPA)), Joshua Novacheck (National Renewable Energy Laboratory (NREL)), Clayton Barrows (NREL), Eric M. Heredia (BPA), Swen Bergman (BPA), Matthew Johnson (BPA), John Kerr (BPA), Clifton Black (Southern Company), Ebrahim Rahimi (CAISO), Matthew Korytowski (Siemens), Milorad Papic (Idaho Power), Daniel P. Pool (BPA), Rebecca Ostash (TransGrid Solutions), Stephen J. Beuning (Xcel Energy) and Sakshi Mishra from American Electric Power (AEP).



## Acronyms and abbreviations

AAC	alternate-arm converter
AC	alternating current
AEP	American Electric Power
BPA	Bonneville Power Administration
CAISO	California Independent System Operator Corporation
CIMWBL	induction motor model in PSS®E
COI	California Oregon Intertie
CPAAUT	frequency sensitive auxiliary signal model in PSS®E
CPS	St. Louis substation
CSEE	Chinese Society for Electrical Engineering
CTL	cascaded two-level
DAE	differential algebraic equations
DC	direct current
DOE	U.S. Department of Energy
DVN	Davenport substation
EI	Eastern Interconnection
ELD	El-Dorado substation
EMS	energy management system
EMT	electromagnetic transient
EMTDC	electromagnetic transients and DC algorithms used in PSCAD software
ERAG	Eastern Interconnection Reliability Assessment Group
ERCOT	Electric Reliability Council of Texas
FDR	frequency disturbance recorder
FRM	frequency response measurement
FRO	frequency response obligation
GaTech	Georgia Tech
GE PSLF	General Electric Positive Sequence Load Flow
GMLC	Grid Modernization Laboratory Consortium
HS	heavy summer
HVDC	high voltage direct current
IAB	industry advisory board
ISO	independent system operators
LCC	line commutated converter
MIESCR	multi infeed effective short circuit ratio
MISO	Mid-Continent Independent System Operator
MMC	modular multilevel converters

MMWG	EI's multi-regional modeling working group
MSP	Minneapolis substation
MTDC	multi-terminal direct current
NERC	North American Electric Reliability Corporation
NREL	National Renewable Energy Laboratory
NY ISO	New York independent system operator
ODE	ordinary differential equation
ORNL	Oak Ridge National Laboratory
PLV	Palo Verde substation
PMU	phasor measurement unit
PNNL	Pacific Northwest National Laboratory
POI	point of interconnection
PSCAD	power systems computer-aid design software
PSS®E	Siemens Power System Simulator
PTDF	Power transfer distribution factors
QSS	quasi steady state
RTO	regional transmission organizations
SDG&E	San Diego Gas and Electric
SFO	San Francisco substation
SM	submodule
SPP	Southwest Power Pool
SRF-PLL	synchronous reference frame phase-locked loop
TGS	TransGrid Solutions
VCV	Victorville substation
VSC	voltage source converters
WAPA	Western Area Power Administration
WECC	Western Electricity Coordinating Council
WI	Western Interconnection
ZIP	constant impedance, constant current and constant power load model

# Contents

Abstract.....	iii
Acknowledgments.....	xvii
Acronyms and abbreviations.....	xix
1.0 Introduction.....	1
1.1 Project objectives, organization and outcomes.....	4
1.2 Relationship to US DOE’s Grid Modernization Laboratory Consortium (GMLC).....	5
1.2.1 Connection to other US DOE GMLC projects.....	5
1.3 Project participants and industry advisory board members.....	6
2.0 Technical Approach.....	7
2.1 Modeling and initial feasibility study in the North American systems.....	8
2.2 Provision of congestion relief and inertial/frequency response with HVDC, in addition to bulk power.....	12
2.2.1 Provision of congestion relief in AC system by HVDC macrogrid.....	12
2.2.2 Provision of frequency and inertial response by HVDC macrogrid.....	12
2.3 High fidelity models of VSC-HVDC.....	16
2.3.1 Modular multilevel converter (MMC).....	16
2.3.2 MMC-HVDC systems: terminal models.....	17
2.3.3 MMC-HVDC systems: EMT model and simulation algorithm.....	19
2.4 Multi-terminal VSC-HVDC control approach.....	21
2.4.1 Outer-loop control system.....	21
3.0 Technical results summary.....	25
3.1 Accomplishments for power flow and transient stability models with the continental-level model.....	25
3.1.1 Model building.....	25
3.1.2 Congestion relief.....	31
3.1.3 Frequency and inertial response.....	33
3.2 Results from high-fidelity modeling and multi-terminal approach.....	41
3.2.1 Validation & comparison of proposed MMC model.....	41
3.3 Multi-terminal VSC-HVDC across EI-ERCOT-WECC.....	43
4.0 Conclusions, lessons learned, and future work.....	47
4.1 Conclusions.....	47
4.2 Lessons learned.....	47
4.3 Future work.....	49
4.4 Final outcome.....	50
4.5 Industry advisory board discussions and feedback.....	50
4.6 Presentations and publications.....	51
5.0 References.....	53

Appendix A Advanced HVDC dynamic modeling..... 57

# Figures

Figure 1: Three main aspects addressed in this project.....	5
Figure 2: Combining the two largest interconnection models .....	9
Figure 3: Load diversity between different regions of US Grid [MISO 2014].....	10
Figure 4: HVDC substation siting procedure.....	10
Figure 5: HVDC macrogrid network, design proposed by [MISO 2014] showing the power flow for the WECC2EI case .....	11
Figure 6: The CPAAUT type HVDC auxiliary signal controller in PSS®E [Siemens PTI 2013] .....	12
Figure 7: Location of FDR for frequency support controller for the HVDC network.....	13
Figure 8: Proposed working principle for autonomous frequency controller .....	14
Figure 9: Example for HVDC macrogrid frequency response.....	15
Figure 10: MISO PMU installation architecture .....	15
Figure 11: Frequency response controller operation methodology.....	16
Figure 12: Circuit diagram of MMC.....	17
Figure 13: Back-to-back MMC-based HVDC system.....	18
Figure 14: Terminal models of MMC-HVDC systems.....	18
Figure 15: Hysteresis relaxation applied to arm currents' dynamics.....	20
Figure 16: Numerical stiffness based separation of modular multilevel converter (MMC) voltage source converter (VSC) dynamic simulation algorithm.....	20
Figure 17: Multi-terminal MMC-HVDC system. ....	21
Figure 18: SM capacitor energy based inertial support to weak AC grids. ....	22
Figure 19: Active power based inertial support. ....	22
Figure 20: Summary of overall control strategy. ....	23
Figure 21: HVDC link configuration .....	26
Figure 22: One-line diagram of the HVDC macrogrid .....	27
Figure 23: Synchronous condenser sizing to support reactive power consumption of HVDC LCC terminals.....	29
Figure 24 MISO model validation result for Fermi Plant trip .....	31
Figure 25 Governor model improvement methodology in EI.....	31
Figure 26: Diagram of transfers analyzed for studying congestion relief in WI (left) and EI (right).....	32
Figure 27: Line sensitivities.....	33
Figure 28: The PTDFs of studied paths within WECC.....	33
Figure 29: Responses of the three HVDC lines with the CPAAUT auxiliary signal controller .....	35
Figure 30: Comparison of the frequency responses for the scenarios with and without the HVDC frequency auxiliary controllers. ....	36
Figure 31: HVDC schedule changes for Grand Gulf trip .....	37
Figure 32 HVDC schedule changes for Palo Verde trip.....	37
Figure 33: HVDC frequency response for Fermi trip .....	38

Figure 34: HVDC frequency response for Grand Gulf trip .....	39
Figure 35: HVDC frequency response for Palo Verde both unit trip.....	40
Figure 36: States of MMC under steady-state: (a) phase-a arm currents, and (b) phase-a average capacitor voltages in each arm .....	42
Figure 37: States of MMC under steady-state: (a) phase-a arm currents, and (b) phase-a average capacitor voltages in each arm .....	43
Figure 38: MMC phase-a arm currents under DC fault condition. ....	43
Figure 39: Multi-terminal MMC-HVDC system connecting three asynchronous grids in US.....	44
Figure 40: Frequency response provided by the MTDC system to support 500-MW loss in ERCOT: (a) Comparison of frequency in ERCOT with and without MTDC, (b) Frequency in EI and WECC with the MTDC support to ERCOT.....	44
Figure 41: Frequency response provided by the MTDC system to support 500-MW loss in WECC: (a) Comparison of frequency in WECC with and without MTDC, (b) Frequency in EI and ERCOT with the MTDC support to WECC. ....	45
Figure 42: Frequency response provided by the MTDC system to support 1000-MW loss in EI: (a) Comparison of frequency in EI with and without MTDC, (b) Frequency in ERCOT and WECC with the MTDC support to EI. ....	46
Figure 43: A comparison of point-to-point LCC layout and multi-terminal VSC layout for the macrogrid.	48
Figure 44: Summary of internal control system.....	61
Figure 45: MMC submodule capacitor voltage balancing algorithm. ....	62

## Tables

Table 1: Case summary of the developed continental-level power flow model .....	27
Table 2: Multi-infeed effective short circuit ratio (MIESCR) .....	28
Table 3: Case summary of the developed macrogrid transient stability model .....	30
Table 4: Results of frequency response measurement for central controller .....	40
Table 5: MMC system parameters .....	41
Table 6: Simulation parameters .....	41
Table 7: Benefits of VSC over LCC .....	49



# 1.0 Introduction

HVDC transmission has growing interest around the world [Liu 2015, Perri 2017, Rao 2015, Xu 2017, Zhou 2016, and Fairley 2016]. This is a result of recent advancements in power electronics technology and the potential value to transfer power between distant regions and off-shore locations. The recent technology advancements include the development of more efficient and compact voltage source converters (VSCs) like the modular multilevel converter (MMC) that was used in the Trans-Bay Cable project in San Francisco. By taking advantage of their flexibility and controllability, high voltage direct current (HVDC) technologies could provide various reliability and economic benefits to the existing electricity infrastructure.

Bulk power transfers through multiple HVDC lines within and across large alternating current (AC) interconnections could have various economic benefits. Economic benefits could range from interregional capacity exchange to take advantage of load diversity, wind and solar diversity, and energy arbitrage [MISO 2014], through improved reliability and additional ancillary-services benefits. These added potential benefits can result from operating several HVDC lines in a coordinated way and in networks configurations, and have not been deeply studied yet [Kirkham 2014].

A comparison of AC and direct current (DC) systems, including characteristics of voltage source converters (VSC-HVDC) systems was provided in a WECC report [Makarov 2013]. This comparison is brought below.

“HVDC system for 750 to 800 kV has been often identified as advantageous for transmitting large power over long distances.” [Huang 2002]

The following advantages of DC systems over AC systems for integration of renewable energy are listed in the available literature:

- Interconnection of non-synchronous systems. [Alstom Grid 2010]
- Multi-terminal DC system configuration helps to increase operation flexibility, availability and reliability and controllability and increase power transfer capability. (Alstom Grid 2010)
- Investment cost. Above a certain distance, the so called "break-even distance", the HVDC transmission provides the lowest cost. [Larruskain et al. 2007].
- Capacitive charging current. The length of AC cables for practical use is limited by the capacitive charging current. HVDC technology has no charging current in the DC cables [Alstom Grid 2010]
- Lower losses. DC transmission losses are up to 40% less comparing to AC. [Green Economy 2011].
- Right-of-way. A DC transmission line requires about a third the right-of-way of that of that needed for a conventional AC transmission line.” [Green Economy 2011]
- Controllability and power modulation capability. An HVDC power can be modulated the power to stabilize the surrounding AC system. [Lescale et al. 2008]

The HVDC systems can also pose some serious negative system impacts and/or design implications that should be taken into consideration:

- The cost of converter stations makes DC lines less cost-effective for short distances.
- Reliability. Due to the large amount of power transmitted by HVDC transmissions reliability is the most important concern in terms of reliability, transient reliability and recovery after temporary faults and disturbances, including the spread of disturbances in multi-terminal DC systems [Lescale et al. 2008]
- DC circuit breakers for DC grid protection is a problem [Alstom Grid 2010]
- “Operation and control strategies for multi-terminal DC grid voltage control, power sharing and dispatch among the connected AC grids, voltage and frequency support of the connected AC grids, etc.” [Alstom Grid 2010]

The characteristics of VSC-HVDC discussed in the WECC report [Makarov 2013] were:

The characteristics of VSC-HVDC have been investigated in [Arrillaga et al. 2007; Asplund 2000; ABB 2012; Zhang 2004], and other papers. These papers are summarized below.

- The key advantages of VSC-HVDC, in comparison with the classic HVDC that is based on current source converters, are described in [Arrillaga et al. 2007, Asplund 2000, and ABB 2012]. VSC-HVDC can control both active and reactive power independently, and generate or consume reactive power within a wider range than a conventional HVDC. This is because VSC-HVDC converter stations employ state-of-the-art power semiconductors. VSC-HVDC can create any voltage phase angle or amplitude almost instantaneously, and operate even at zero active power, and still provide the full range of reactive power. VSC-HVDC is based on a modular concept with standardized sizes for the converter stations. The converter station with VSC is more compact and has a smaller footprint. Modular systems can be installed in different stages to meet the capacity demand. VSC-HVDC allows connecting substations to a generic point of the line. Costs are naturally lower when the new substation is not sized to carry the full load. VSC technology facilitates the connection of several converters to a common bipolar DC bus because the voltage polarity is not reversed when changing the power direction.
- The VSC-HVDC technology also presents some drawbacks when compared to conventional HVDC. As a result of higher cost of the converter stations, VSC-HVDC technology is more expensive than traditional LCC HVDC. VSC-HVDC technology shows higher converter losses than traditional HVDC. Consequently, for a given transmission capacity, the cable length that equals the AC overhead line systems losses is higher than that for HVDC. VSC-HVDC is by nature bipolar because the DC circuit is not connected to ground. Differently from traditional bipolar HVDC, VSC-HVDC has no possibility to execute emergency power transfer via one pole when the other pole trips. DC line-to-ground faults are more critical with VSC-HVDC. However, considering the intrinsic features of VSC-HVDC and the steady advances in such technological fields, it is expected that some disadvantages can be quickly scaled down and others overcome.

Several proposals for HVDC macrogrids exist for Europe [Perri 2017] and for the North American continental-level interconnections [MISO 2014, Kirkham 2014, McDonald 2016, and Li 2015]. Multiple HVDC infeed between regions have been recently built in Southern China grid [Zhou 2016 and Fairley

2016]. The economic benefits of one particular configuration in North America were conceptually evaluated in [MISO 2014]. 45% of the total economic benefit was estimated by the authors of that study to be drawn from taking advantage of load diversity between regions in North America.

The HVDC macrogrid configurations for North America, mentioned above, represent significant modification to the grid at a continental level. Economic and technical evaluation of these HVDC macrogrid proposals have only been performed at a conceptual level. Detailed power-flow and transient stability studies have not been performed. These types of studies are key for the engineering community to understand the technical feasibility of such HVDC configurations. This study makes progress towards demonstrating technical feasibilities of one HVDC macrogrid configuration. In addition, this study shows how HVDC lines can also be used to provide additional benefits, like frequency response and congestion management.

The HVDC macrogrid configuration adopted in this study comes from Mid-Continent Independent System Operator's 2014 planning study [MISO 2014]. Total transfers of 14.4 GW between Eastern and Western Interconnections in North America are examined. Another parallel effort [NREL 2017] considering HVDC macrogrids focuses on detailed economic benefits of various configurations and initial power flow studies for the most economic option. Complementary to [NREL 2017], this study focuses on the power-flow and dynamic studies to show the initial feasibility of HVDC and multi-terminal DC (MTDC) configurations, and on the modeling of advanced configurations such as the VSC MMC, and MTDC networks.

The technologies required in a HVDC macrogrid or in an incrementally embedded DC system in AC interconnections are not completely known at this moment. One of the reasons for this is the rapid development of VSC topologies and DC breakers. Some of the recent VSC topologies include MMC, cascaded two-level converter (CTL), and the alternate-arm converter (AAC). The MMC configuration, in particular, is at an advanced stage of commercialization. It has become an attractive VSC topology in HVDC transmission systems due to its attractive features like low harmonics, modularity, and scalability [Debnath 2015]. Modeling and simulation of MMCs is challenging due to the complex circuit configuration present. The high-fidelity models of MMCs are absent in standard simulation software today. This project develops open-source high-fidelity models and simulation algorithms for fast and accurate analysis of the dynamics of MMC. The developed simulation algorithm is also applied to MMCs in point-to-point DC and MTDC configurations.

This project covers two approaches for modeling:

1. Modeling large continental power system based on current industry-accepted models of the large interconnections and of the HVDC lines, building for the first time a power-flow and transient stability, continental-level model of North American Eastern and Western Interconnections, interconnected through HVDC lines with significant transfers
2. High-fidelity modeling of advanced HVDC configurations, VSC MMC, in point-to-point and multi-terminal topologies
3. Future work of this project will combine models in 1 and 2.

The value propositions of this project are:

- Enable decision-makers and investors to make well-informed and significant decisions regarding the DC systems as an important grid development option.

- The multi-objective control and DC models developed in this project target solutions to current and future RTOs/ISOs/utilities' HVDC systems.
- Develop accurate models of DC technologies and explore multi-objective DC control methods.
- Maximize the benefit of DC systems as they overlap with the AC systems by using their flexibility to provide much-needed services to the grid at the same time as moving blocks of energy.
- Demonstrate feasibility and reliability of such systems.
- Use cases in which DC lines will be controlled to support healthy values of AC power transfers, provide ancillary services, and prevent instabilities.
- Study the technical benefits of HVDC system embedded in AC interconnections and interlinks between AC interconnections.

## 1.1 Project objectives, organization and outcomes

The main objective of this project is to develop the models and methods for assessing the impact of DC technologies, embedded and across large interconnected AC systems. The main outcomes in the first year of this project have been:

- ✓ A first-ever full-size AC-DC dynamic model for Eastern and Western Interconnections, and developed used cases.
- ✓ Accurate models of DC technologies and explore multi-objective DC control methods.

Initial focus of the analysis and modeling was made on congestion relief and frequency/inertial response services, being provided at the same time as bulk power transfers. Other services will be considered in follow on work. The main reason to focus on congestion relief is to take advantage of the following benefits:

- Reduce congestion costs: The congestion cost can reach billion dollars a year, e.g., for New York independent system operator (NY ISO) - \$1.5 billion in 2008; California ISO - \$1 billion for 2004.
- Allow transmission grid to operate closer to the maximum limits.
- Address growing uncertainty, stochastic power flow patterns and loop flows pressing the transmission system's ability to maintain high reliability and continued affordability of power delivery to the limit.

While, frequency/inertial response improvement could bring about the following benefits:

- The value of frequency response: (1) avoid penalties related to frequency response obligation (FRO); (2) FRO sharing benefits; (3) Sharing contingency reserves; (3) Prevent load and generation disconnections; and (4) Prevent cascading outages and blackouts.

- Benefit comes from [MISO 2014]:
  - \$700,000/MW from capital cost of capacity
  - \$13/MWh from frequency response premium.

## 1.2 Relationship to US DOE’s Grid Modernization Laboratory Consortium (GMLC)

Under the US DOE’s Grid Modernization Laboratory Consortium (GMLC), this project is under the area of Design and Planning Tools, particularly for HVDC and MVDC analysis.

As the generation mix changes and shifts in location, HVDC and MVDC may play a greater role in the future grid. Currently, the models and methods for assessing the value of these technologies have been limited. This activity will improve models and focus on exploring scenarios and use cases, such as accelerated siting from undergrounding and the provision of virtual inertia. This activity may be combined with other analysis to explore system flexibility more holistically.

In this project we address models and methods needed for multi-objective control of HVDC and MVDC. The following diagram (Figure 1) shows the three main aspects addressed in this project, in its first year.

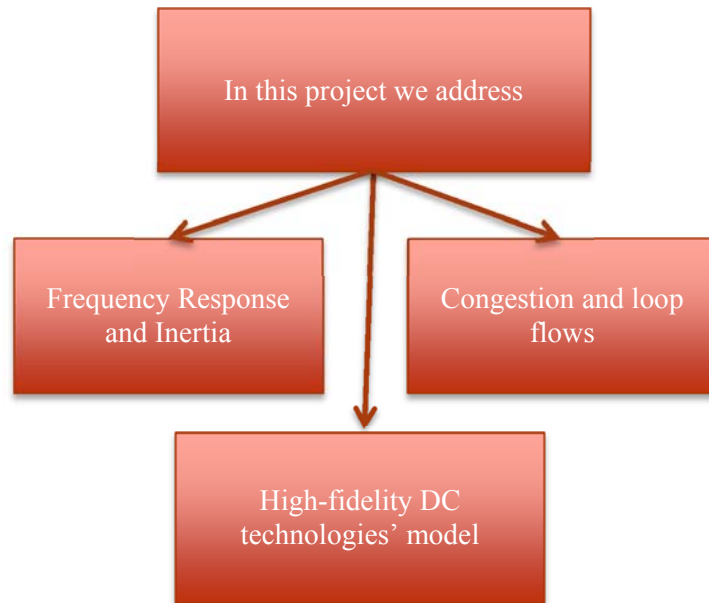


Figure 1: Three main aspects addressed in this project

### 1.2.1 Connection to other US DOE GMLC projects

This project is connected to three other efforts under US DOE’s GMLC.

This project is linked to GMLC Category 1 Midwest Regional Partnership project 1.3.33 “The Interconnection Seams Study”, which aims to study the HVDC and AC transmission seams between the U.S. interconnections and propose upgrades to existing facilities that reduce the cost of modernizing the nation’s power systems. This project is an incremental effort to increase the value of HVDC connecting ties by adding essential grid reliability services to just moving blocks of energy from the Eastern Interconnection to the Western Interconnection and vice versa, as suggested in GM 1.3.33.

This project can also leverage findings with project GM0073 “HVDC and Load Modulation for Improved Dynamic Response using Phasor Measurements.” Part of project GM0073 covers control of three or more HVDC lines (current system with minor modifications) in an AC interconnection to damp interarea oscillations. This is developed initially at a conceptual level in GM0073. There could be a possibility to leverage work in GM0073 and GM0074.

This project can also achieve coordination with GMLC 1.4.18 “Computational Science for Grid Management,” because the challenge of modeling advanced HVDC systems and the scalability needed in continental level models could potentially need the advanced computational and solvers used in GMLC 1.4.18.

### **1.3 Project participants and industry advisory board members**

The project team is formed by national laboratories and industry, whose members effectively collaborated with significant results in short time. The project team organized biweekly teleconference meetings to coordinate work across institutions. The authors of this report were joined by American Electric Power (AEP) and Southwest Power Pool (SPP) in the biweekly meetings.

The project team presented intermediate progress to an industry advisory board (IAB). The IAB assisted the national laboratories with building the accurate realistic cases for simulations. IAB provided feedback on scenarios of study, use cases, and events of interest. There were three IAB meetings with participants from the following institutions: California Independent System Operator (CAISO), Xcel Energy, Western Area Power Administration (WAPA), San Diego Gas and Electric (SDG&E), Bonneville Power Administration (BPA), Idaho Power, Georgia Tech (GaTech), TransGrid Solutions (TGS), National Renewable Energy Laboratory (NREL), Southwest Power Pool (SPP), Siemens, Midcontinent Independent System Operator (MISO), ORNL, and PNNL.

## 2.0 Technical Approach

To study the modeling and control of HVDC and MTDC configurations, this project concentrates on two main perspectives of the problem: 1) the feasibility of a continental-level HVDC macrogrid in North America and the potential of such macrogrid to provide the various benefits, concentrating first on congestion management and frequency response, and 2) high fidelity modeling for advanced HVDC configurations and converter designs that could be used in such interconnections to obtain maximum benefits from HVDC lines.

The specific elements of the methodology adopted in the study are:

- Building, for the first time, a continental-level power system model of the Eastern and Western North American power system for power flow and transient stability, interconnected through several HVDC lines. As the first step, modeling is based on industry accepted models, for power flow and transient stability studies, of the Western and Eastern interconnections, as well as industry accepted HVDC line models
- With the continental-level North American power system model, this work explores multi-objective control of HVDC macrogrid. In this first year, the work focused on provision of congestion management and frequency response, in addition to the bulk transfer of energy between regions
- Modeling of advanced HVDC converters, like the modular multilevel converter (MMC), have several challenges because of the complex circuit configurations. Advanced simulation algorithms are required for studying the dynamics of a hybrid (AC-DC) transmission grid with a high penetration of MMCs. This work has developed high fidelity models and advanced simulation algorithms to understand the dynamics of MMC.
- AC and DC terminal models of advanced HVDC converters are developed to interface them with AC and DC system dynamics in point-to-point DC and MTDC configurations. The extension of the developed simulation algorithm is applied to the point-to-point DC and MTDC configurations.
- Develop DC control strategies and the corresponding control strategies of the HVDC/MVDC converters for multi-objective controls to extract the maximum value from the DC systems in different use cases.
- Test multi-objective HVDC/MVDC converter control strategies using dynamic power system models. Identify the impact on grid reliability and performance. Investigate the impact of HVDC converter control strategies on the DC system.

Sections 2.1, 2.2, and 2.3 describe the methodologies in more detail.

## 2.1 Modeling and initial feasibility study in the North American systems

The three large scale power system interconnections in North America (Eastern, Western, and ERCOT interconnections<sup>1</sup>) are studied with separate models, mainly because the systems are decoupled, only connected through relatively small back-to-back interconnections. For the objectives of this project, the large scale interconnections become significantly stronger, and those interconnections are dynamically linked to capture additional benefits.

Therefore, this project builds, for first time, a continental-level power system model of the Eastern and Western North American power system for power flow and transient stability, interconnected through several HVDC lines. As a first step, modeling is based on industry accepted models, for power flow and transient stability studies, of the two largest interconnections (Western and Eastern), as well as industry accepted HVDC line models.

The detailed, industry-grade, interconnection-wide power-flow of Western and Eastern interconnections, built in this project has the following three main components:

- WECC 2025 heavy-summer planning case, provided and built jointly by utilities in the Western Interconnection and WECC
- Eastern Interconnection 2026 summer-peak model, provided by the multi-regional modeling working group of Eastern Interconnection Reliability Assessment Group (ERAG-MMWG)
- Power flow and transient stability models of HVDC macrogrid were built
- Models of Eastern and Western Interconnections were connected through HVDC macrogrid model for power flow and transient stability studies (Figure 2)

---

<sup>1</sup> A simplified model of ERCOT was used in this study.

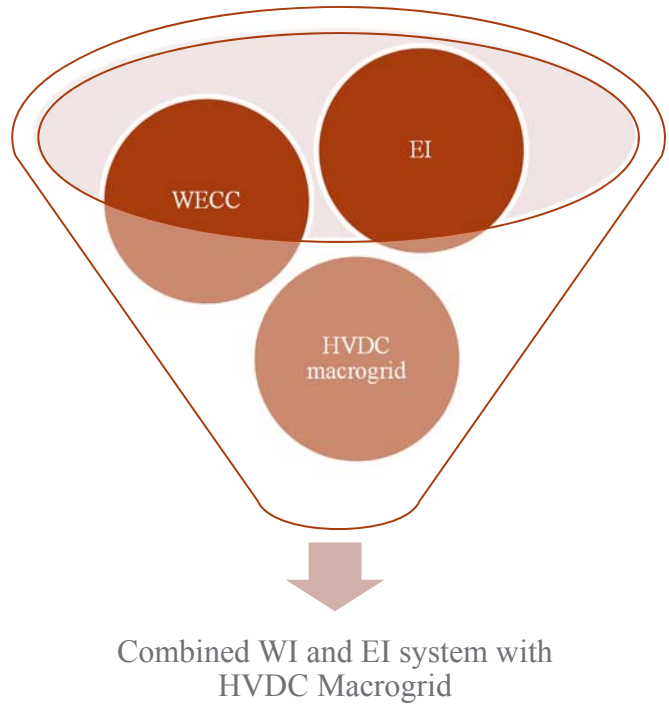


Figure 2: Combining the two largest interconnection models

The HVDC macrogrid was represented by a network of 14 point-to-point line commutated converter (LCC) HVDC systems with a shared AC bus. The HVDC macrogrid power-flow and transient-stability models were built using industry-grade models, and their preliminary parameters were selected using engineering judgement based on distances, levels of transfer, and desired losses; however, the design was not fully optimized. The study conducted by MISO in 2014 envisioned a  $\pm 600\text{kV}$  multi-terminal DC network with LCC and voltage source converter (VSC) technology. This project used a meshed HVDC topology consisting of  $\pm 800\text{ kV}$  two-terminal LCC HVDC technology, which had a maximum transfer capacity of 14.4 GW between the Eastern and the Western Interconnections.

Power transfer scenarios were selected to represent one of the main components of benefit to the HVDC macrogrid proposed by Midcontinent Independent System Operator (MISO) in a study of 2014 [MISO 2014]. This load diversity benefit alone was estimated to provide 45% of the economic benefits. This application required an estimated total of 35 GW transfers (17.5 GW in each direction) between three regions of the West and two regions of the East, as shown in the Figure 3.

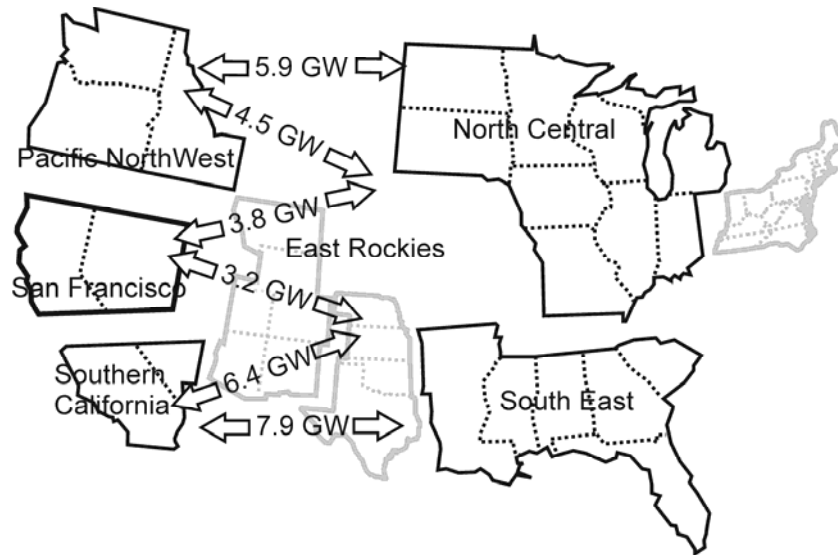


Figure 3: Load diversity between different regions of US Grid [MISO 2014]

To capture load diversity application, large power transfers of 14.4 GW, in each direction, between Eastern Interconnection (EI) and Western Interconnection (WI) were incorporated in the continental-level model, EI and WI, and connected through HVDC macrogrid. This was a significant effort because generation and loads in EI and WI were modified according to industry practices. Typically expensive generation for peak loads was turned off to absorb power in one interconnection, while load was modified to represent a slightly off-peak condition, corresponding to when the transfers were expected to occur. This was an iterative process where overloads in the existing AC infrastructure were corrected by modifying schedules of HVDC and changing HVDC tie-in buses to nearby stronger buses, if needed, as illustrated in Figure 4.

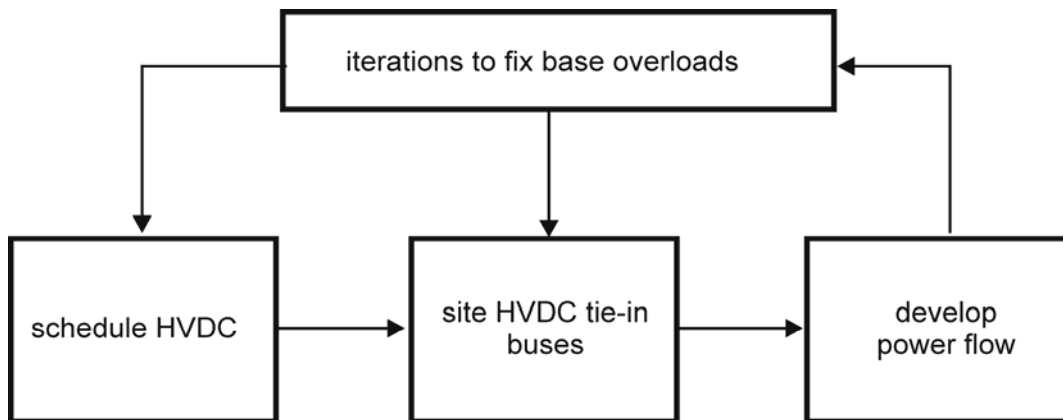


Figure 4: HVDC substation siting procedure

Two transfer scenarios were built, with WI exporting 14.4 GW to EI, denoted as WECC2EI case, and another case with reversed transfers, EI exporting 14.4 GW to WI, denoted as EI2WECC case. For the WECC2EI case:

- WECC in high summer peak conditions had load reduced by 14 GW to model a slightly off-peak loading condition.

- EI: 14 GW of peaking generation was turned off.

While for the EI2WECC case (illustrated in Figure 5):

- WECC: 14 GW of peaking generation was turned off.
- EI generation was the same as high summer peak case, and load was reduced by 14 GW.

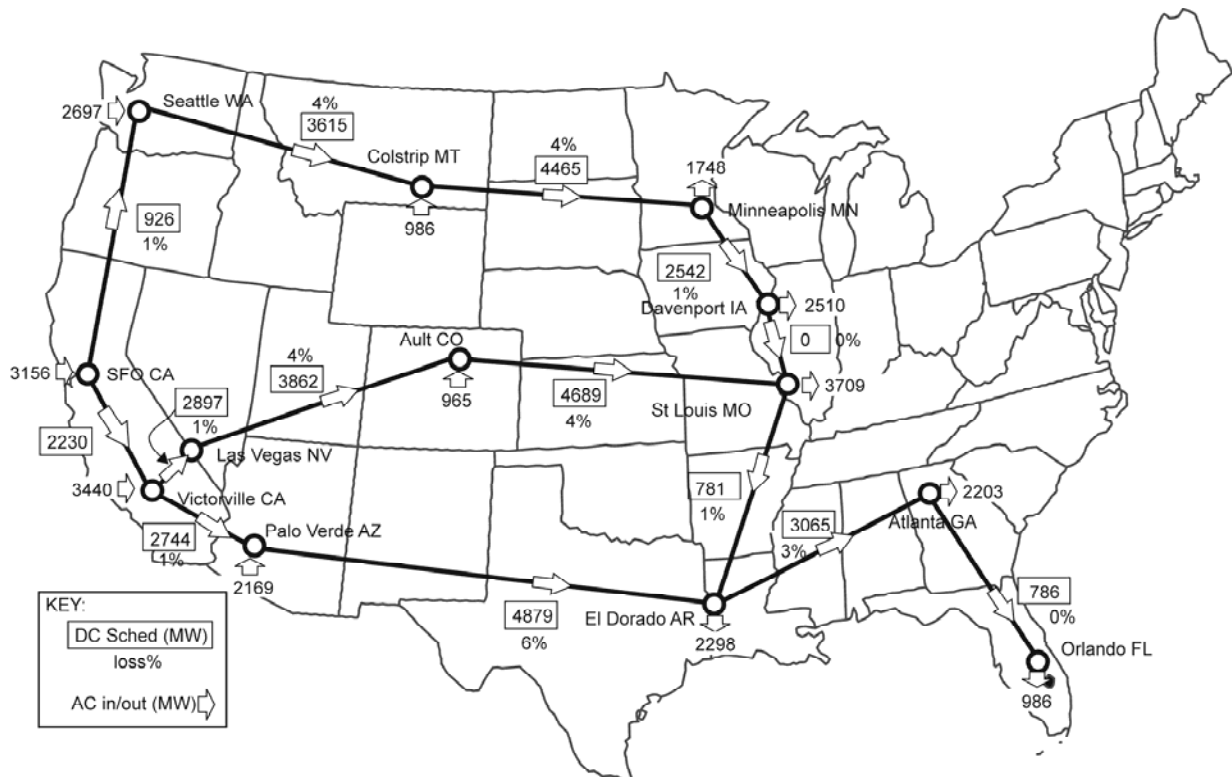


Figure 5: HVDC macrogrid network, design proposed by [MISO 2014] showing the power flow for the WECC2EI case

Additionally, full-size dynamic models of EI and WECC were tested and adjusted for correct initialization and performance for the new system conditions.

For transient stability analysis, a dynamic model for HVDC macrogrid was built. HVDC macrogrid transient stability model was based on industry accepted models and the parameters were selected to represent typical values. This model was combined with the power flow model and tested for acceptable performance. Finally, the HVDC macrogrid power flow and dynamic model were combined with the full models of EI and WECC.

## 2.2 Provision of congestion relief and inertial/frequency response with HVDC, in addition to bulk power transfer

Using the continental-level model described in Section 2.1, use cases were created for congestion relief and frequency/inertial response studies, in addition to bulk power transfers, to EI and WE systems by controlling the HVDC macrogrid.

### 2.2.1 Provision of congestion relief in AC system by HVDC macrogrid

The HVDC macrogrid has several points of injection to the AC interconnections, as shown in Figure 5. The level of injections in those points is controllable by the HVDC converters. The power schedules of the HVDC macrogrid could be modified to relieve congestion and loop flows in the AC interconnections.

To show the capability of mitigating loop flows and congestion relief, this study used two types of simulations in the WECC and in the EI:

1. Study of sensitivity for transferring 2000 MW between two regions in EI, with and without HVDC (part of macrogrid). The sensitivity was calculated using three full power flow cases: a) an initial base case to provide a reference and seed; b) case with an increase of 2000 MW transfer from South region to North region through scaling load and re-dispatch of generators; and c) case with 2000 MW power transfer through an HVDC line.
2. Study congestion relief by making relatively small changes in the HVDC macrogrid schedules between two points of connection within the WECC. The effect of this change of schedule was studied in each commonly monitored transmission path in the WECC. Power transfer distribution factors (PTDF) with respect to HVDC injections were used in this study.

### 2.2.2 Provision of frequency and inertial response by HVDC macrogrid

Two complementary approaches for provision of frequency and inertial response were studied: A localized scheme with immediate response, and a centralized response with slower response, but still fast enough to influence part of the frequency response. The localized response uses controllers in line with current industry practice, while the centralized controller is proposed at the conceptual level.

#### 2.2.2.1 Localized frequency/inertial response scheme

A localized scheme for frequency control from the HVDC lines across the seams between WECC and EI systems has been investigated. In this scheme, the HVDC power schedule is adjusted based on the local frequency deviation, which is realized by equipping each pole of three HVDC systems crossing the interconnection boundaries with the frequency sensitive auxiliary signal model called CPAAUT, as shown in Figure 6.

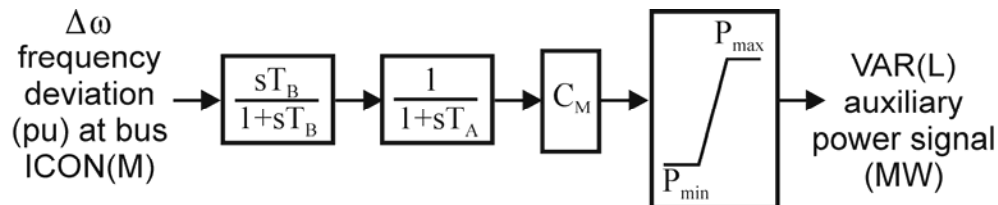


Figure 6: The CPAAUT type HVDC auxiliary signal controller in PSS®E [Siemens PTI 2013]

For the EI to WECC power transfer scheme, the settings of  $T_A = 0.1$  s,  $T_B = 1000$  s,  $C_M = -120000.0$  MW/pu (i.e., 2000 MW/Hz) are used. The frequencies of the HVDC converter AC buses within WECC are employed as input for the HVDC auxiliary signal controller. Because of different frequency response characteristics in the EI system, the  $C_M$  is set to 1200000 MW/pu (i.e., 20000 MW/Hz) when the frequencies within EI system are employed as input to the HVDC auxiliary signal controller.

The response of this localized controller is immediate because the frequency changes as a result of a large event. To assist with slower response, a centralized controller was envisioned.

### 2.2.2.2 Concept for centralized controller for frequency response

A concept of a centralized controller for frequency response at a slower time frame was envisioned to complement the response of localized controller. This centralized controller is envisioned to be automatic, and respond in a time frame that is faster than traditional manual reschedules, and still slower than an immediate response of localized control, such as the one described in Section 2.2.1.

The proposed centralized controller could be deployed with a dedicated network of time synchronized frequency disturbance recorders (FDR) monitors or phasor measurement units (PMU) at each of the HVDC macrogrid point of interconnection (POI), which would connect to the central controller located in Ault, Colorado, as shown in Figure 7.

The location of the central controller was envisioned to minimize data latency. The dedicated communication channels usually installed in long distance HVDC links may be utilized by the centralized controller. This could represent a potential cost saving, and the fact that these communication channels are dedicated to the HVDC lines can provide for a degree of reliability and security.

Figure 8 describes the working principle of the HVDC wide-area based frequency controller.

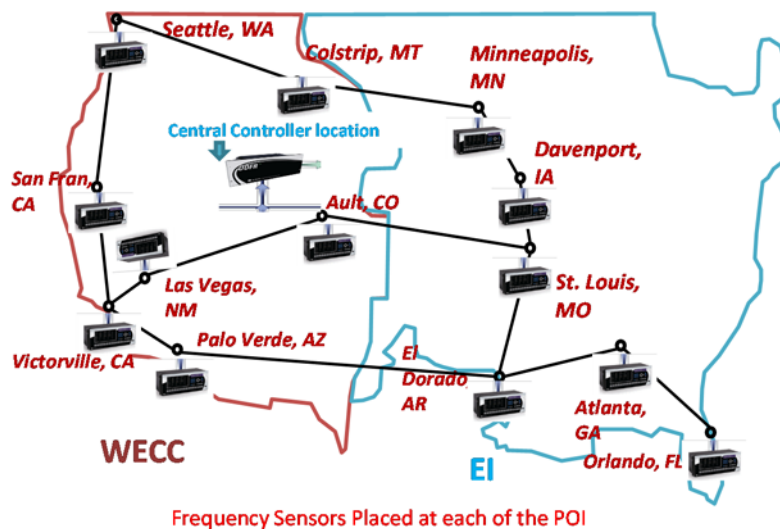


Figure 7: Location of FDR for frequency support controller for the HVDC network

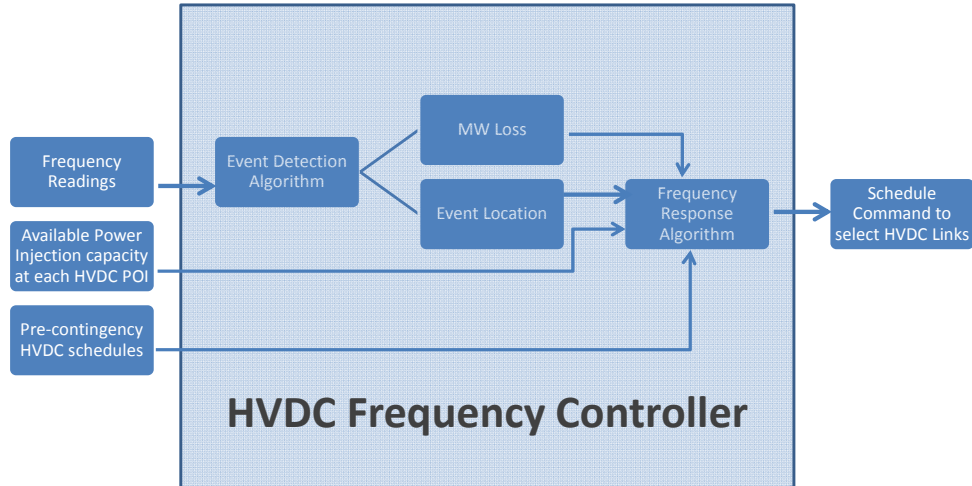


Figure 8: Proposed working principle for centralized frequency controller

Frequency readings from the FDR or PMU, HVDC schedules and available power injection capacity from each of the HVDC POI are the inputs to the central controller. Using a triangulation technique such as the technique based on wave arrival or least square method [Xia 2017], the central controller could estimate the event location and MW loss.

Once the event location and size of MW loss is known, the central controller could schedule the best combination of power flows on each HVDC line of the macrogrid, to optimize the overall response. For example, the controller could determine the HVDC macrogrid's node nearest to the event location, which is the most suitable to provide frequency support. The HVDC lines could be scheduled to deliver the response to that particular node.

The controller could take into account several factors before arriving to the final schedules for the HVDC macrogrid. Such factors could be event location and size of generation or load loss, knowledge of pre-contingency HVDC schedules, available power injection capability from HVDC nodes in the pre-contingency grid.

To illustrate the concept, consider the following example. Suppose the event detection algorithm successfully identifies a loss of 590 MW generators near the St. Louis HVDC POI in a transfer case when WECC is supplying power to EI, as shown in Figure 9. In this example, only three of the WECC POIs (namely Seattle, San Francisco, and Palo Verde) are assumed to have available capacity of 200 MW at each location. Other locations in WECC footprint are assumed to have no capacity in that instant. The frequency controller will increase the HVDC schedules of the three West to East HVDC links by 200 MW. A net injection of 600 MW from WECC is considered, assuming there will be some losses over the HVDC links. The central controller will also change the schedule of the North-South HVDC links in the EI such that the frequency support is pinpointed towards the disturbance area, which is close to St. Louis in this example. In Figure 9, the orange arrows show the path of power flow for frequency response support.

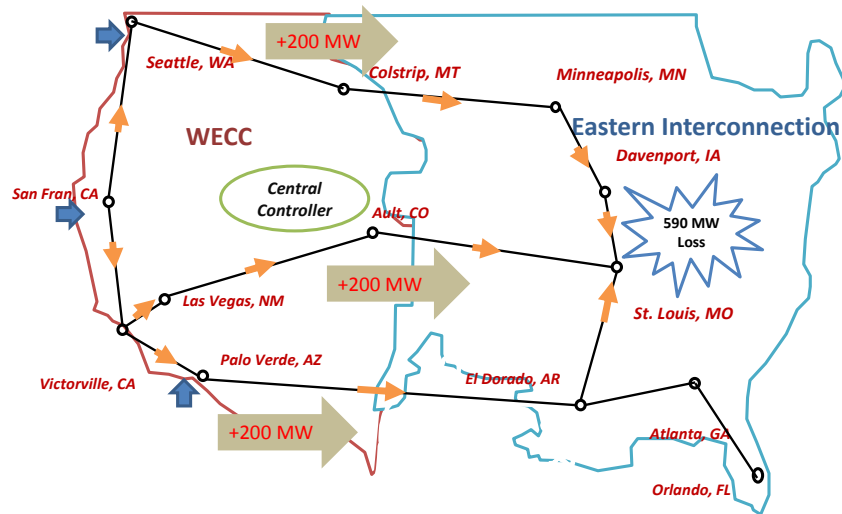


Figure 9: Example for HVDC macrogrid frequency response

It should be noted that the methods described in [Xia 2017] calculate coordinates within 100 miles of the actual event location and requires several seconds to perform the calculations because of data latency and sampling window required for determining the event detection. However, utilizing the communication network architecture similar to the MISO's PMU installation, as shown in the Figure 10, the action of central controller could potentially be performed faster.

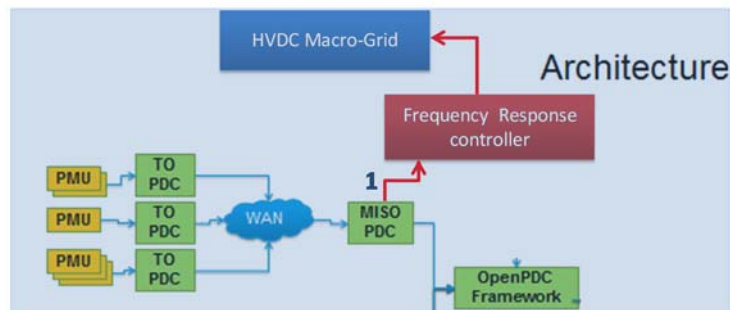


Figure 10: MISO PMU installation architecture

The central controller could be designed to support frequency response characteristics of the Eastern Interconnection and WECC for the later period of the frequency response. The frequency nadir in EI is typically attained within 8~10 seconds post trip of a generating plant [BAL-003-1 2008]; however, the controller should react immediately to affect the frequency nadir. A localized controller like the controller discussed in Section 2.2.1, with immediate response, could be used for this purpose. On the other hand, the proposed centralized controller could help with the later part of the response. To support this period in the Eastern Interconnection, the HVDC controller action should start within 2-3 seconds. The HVDC schedule may be changed based on a predetermined ramp over several seconds, as shown in the Figure 11.

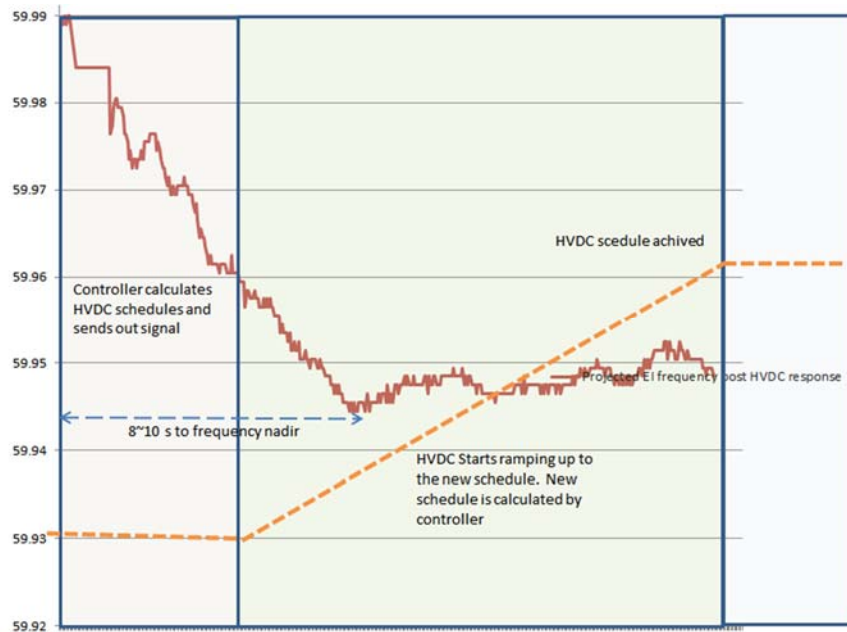


Figure 11: Frequency response controller operation methodology

Finally, the centralized controller may be designed with a dead-band to ignore frequency excursion of smaller values, which may be supported by local resources. And a “no-response” list be could be deployed to make sure that the HVDC macrogrid does not respond to events outside of participating utilities.

## 2.3 High fidelity models of VSC-HVDC

High-fidelity modeling like the electromagnetic transient (EMT) modeling is required to understand the dynamics of weak AC grids, technologies with fast dynamics, systems with increased penetration of renewables, and others. With increased penetration of DC and renewables, EMT modeling will play an increasingly important role.

The EMT modeling of an MMC, as well as MMCs in point-to-point DC and MTDC configurations, is challenging because of the complex circuit configuration of the MMCs. The complex circuit configuration leads to the presence of a large number of states in the systems.

### 2.3.1 Modular multilevel converter (MMC)

A circuit diagram of a half-bridge based MMC is shown in Figure 12. The MMC consists of three phase-legs. Each phase-leg consists of two arms: the upper arm and the lower arm. Each arm consists of “N” series connected submodules (SMs) and an inductor, where “N” is in the range of several hundred today and can range up to a few thousands in the near future for HVDC applications. Each SM can be a half-bridge, full-bridge, clamp-double, and other three-level and fault-tolerant configurations [Debnath 2015]. Based on the SM configuration, the number states within each MMC can vary between “6N+6” in half-bridge based MMCs to “12N+6” in clamp-double-based MMCs. The states are calculated based on the number of capacitor voltages and inductor currents present in the MMC. From the calculated states, it can be observed that within an MMC-HVDC, several thousands of states are present. Moreover, the presence of a large number of diodes introduces numerical stiffness in the simulation model of the MMC. The presence of such a large number of states, the requirement of small simulation time-steps to accurately

capture the harmonics present in such systems, and the numerical stiffness in the simulation model result in the aforementioned advanced simulation requirements.

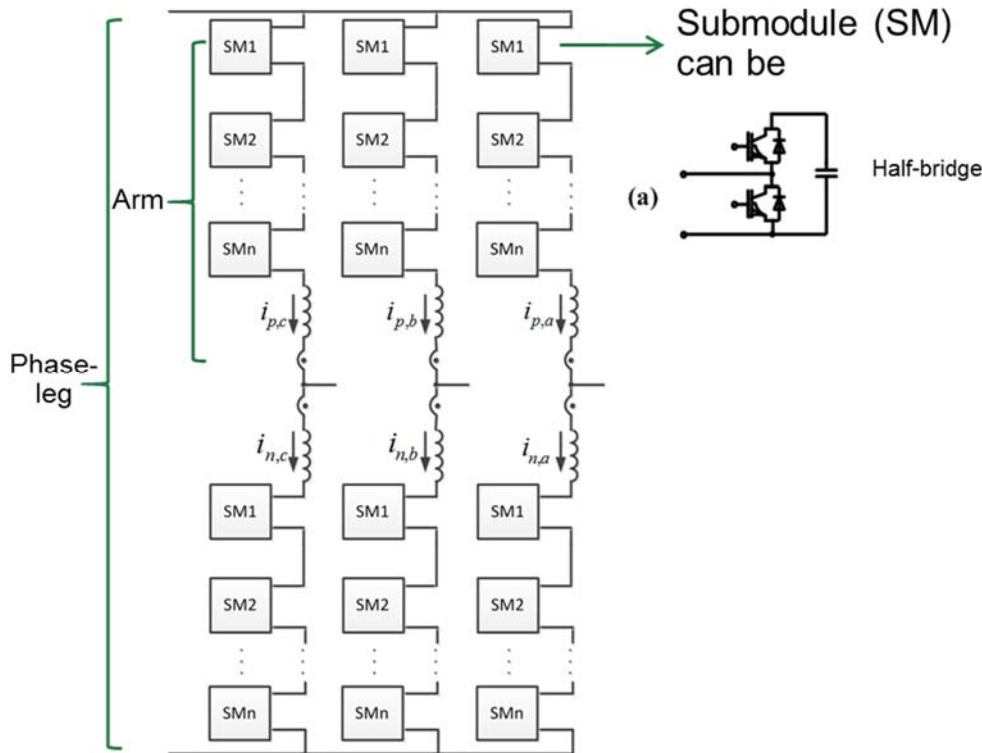


Figure 12: Circuit diagram of MMC.

In this work, models of MMCs based on half-bridge SMs are being developed to efficiently simulate large hybrid transmission grids. Only half-bridge SMs are considered because of their popularity over other SM configurations. The models developed in this work are based on the formulation of the differential algebraic equations (DAEs) that describe the dynamics of the system. The developed models are separated based on stiffness and time-constants to allow hybrid discretization and multi-rate simulation that reduce the computational burden imposed. The hybrid discretization algorithm is based on explicit and implicit discretization algorithms without and with stiff-decay properties, respectively. To enhance the stability of the separated systems, relaxation algorithms are applied to the interfaces created between the separated systems.

### 2.3.2 MMC-HVDC systems: terminal models

An example of a MMC-based HVDC system is shown in Figure 13. The MMCs shown in the figure are represented by the circuit shown in Figure 12. The three slanted lines and two slanted lines in Figure 13 represent three-phase AC overhead lines and DC overhead lines (or cables), respectively. The DAEs formulated for this system can be separated based on time-constants under the assumption that the AC and DC lines are sufficiently long. The long AC and DC lines will have much larger time-constants compared to the dynamics of the MMC. This assumption is particularly valid in a HVDC macrogrid scenario that is being planned to link the Eastern and Western Interconnection. The separated DAEs can be equivalently represented by the circuit shown in Figure 14. The terminal voltage sources shown in Figure 14 are based on the voltage-behind-reactance model that allows stable separation based on time-constants. Because VSCs are being considered as the power conversion systems, the voltage-behind-reactance models have been used for the development of the terminal models in the power conversion

systems. The VSCs control the current in the AC and DC sides through the control algorithms implemented and hence, the current-source based terminal models have been implemented in the AC and DC systems. The cables or overhead lines shown in Figure 14 are implemented based on a distributed RLC traveling wave model (frequency dependent model) [Morched 1999, Gustavsen 1999]. The aforementioned models represent the full frequency dependence of a transmission system, thereby capturing the dynamics accurately.



Figure 13: Back-to-back MMC-based HVDC system

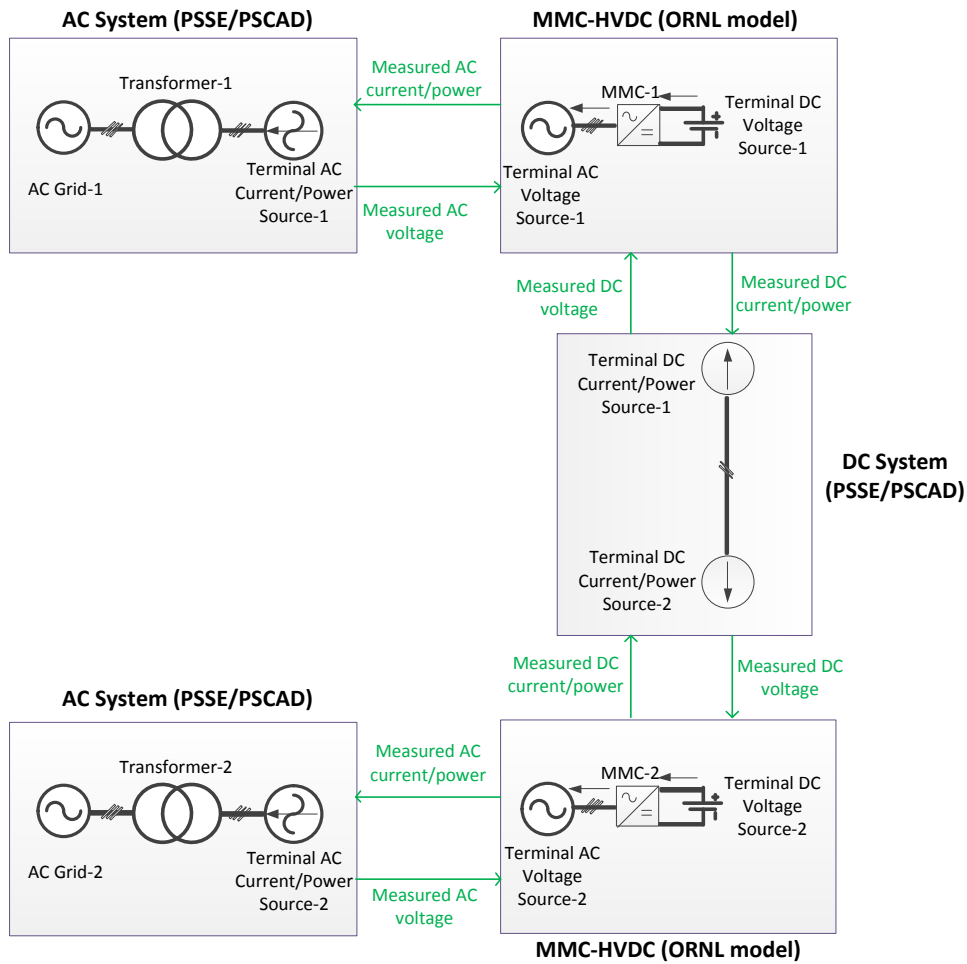


Figure 14: Terminal models of MMC-HVDC systems

In the case of aggregated AC grid models, the AC systems in Figure 14 can be neglected and the terminal AC voltages can represent the AC grid models. Aggregated AC grid models are models where loads and sources are aggregated and placed as a three-phase AC voltage source with three-phase reactors.

The developed terminal models allow the implementation of hybrid discretization and multi-rate algorithms to simulate the AC and DC transmission systems. For instance, the AC and DC systems can be discretized using the trapezoidal method with a time-step of the order of several tens to hundreds of microseconds (or higher based on the time-scales being studied in the power system networks). The trapezoidal method is used to ensure stability of and high accuracy in the simulation of the AC and DC systems [Dommel 1969]. The MMC-HVDC electromagnetic transient (EMT) model can be discretized using a combination of stiff and non-stiff decay algorithms with a time-step of the order of a few microseconds, which will be explained in the following section.

The developed terminal models can be implemented in various HVDC configurations: back-to-back, radial multi-terminal, and meshed multi-terminal. Several of the aforementioned configurations may be noticed in the planned HVDC macrogrid across the Eastern and Western Interconnections as well as in several other HVDC systems being planned in United States. The terminal models integrated with the power conversion system models will be tested in several use cases that include back-to-back MMC-HVDC systems and radial multi-terminal MMC-HVDC systems.

### 2.3.3 MMC-HVDC systems: EMT model and simulation algorithm

*MMC-HVDC Model:* The EMT model of half-bridge based MMC-HVDC system captures the dynamics of the  $6N+6$  states present. The states captured include the  $6N$  capacitor voltages and the 6 arm currents. The arm currents' and capacitor voltages' dynamics are shown by the DAEs in the Appendix A. There is numerical stiffness observed in the arm current dynamics.

The separation of the arm currents' dynamics from the capacitor voltages' dynamics can be easily achieved using an explicit discretization algorithm. However, because of the numerical stiffness observed, explicit discretization cannot be applied to both the dynamics. The proposed separation of the dynamics is based on numerical stiffness and a hysteresis relaxation algorithm.

*Hybrid Discretization Algorithm:* The numerical stiffness is observed only in the arm currents' dynamics as the  $\text{sgn}$  function in the capacitor voltages' dynamics can be treated as an external input. That is, the arm currents' dynamics given in equation (A.1.1), Appendix A, can be discretized using backward Euler, which has stiff-decay property [Gnanarathna 2011]. The capacitor voltages' dynamics in equation (A.1.2), Appendix A can be discretized using forward Euler, which is an explicit discretization algorithm. The use of hybrid discretization results in inverting only a  $5 \times 5$  matrix at every instant in the simulation of the proposed MMC model. In the commercial software and most of the existing MMC models [Gnanarathna 2011, Saad 2014], the simulation of MMC will require the inversion of a  $(6N+5) \times (6N+5)$  matrix. Thus, the computational burden imposed by the simulation of the proposed MMC model is significantly reduced.

An interface is created to exchange information between the two dynamics as arm currents' dynamics depends upon the state of the capacitor voltages and vice-versa. A hysteresis relaxation algorithm is applied at the interface for stable simulation across different external conditions.

*Hysteresis Relaxation Algorithm:* To reduce the numerical stiffness and for ease of discretization, a hysteresis loop is defined for  $\text{sgn}$  function term in Equation (1) in the Appendix A, as shown in Figure 15.

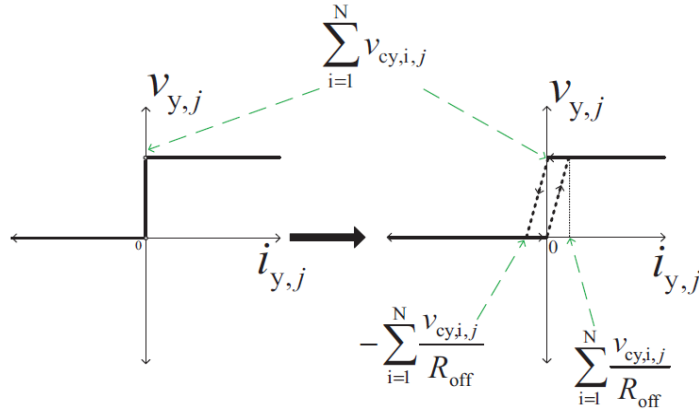


Figure 15: Hysteresis relaxation applied to arm currents' dynamics.

Although the hysteresis relaxation reduces the numerical stiffness in the arm currents' dynamics, the arm currents' dynamics still require an implicit discretization with stiff decay property like backward Euler. The use of backward Euler discretization allows a higher slope in the hysteresis loop that increases the accuracy of the simulation and avoids the requirement of very low time-steps (on the order of nano-seconds).

The overall summary is shown in Figure 16.

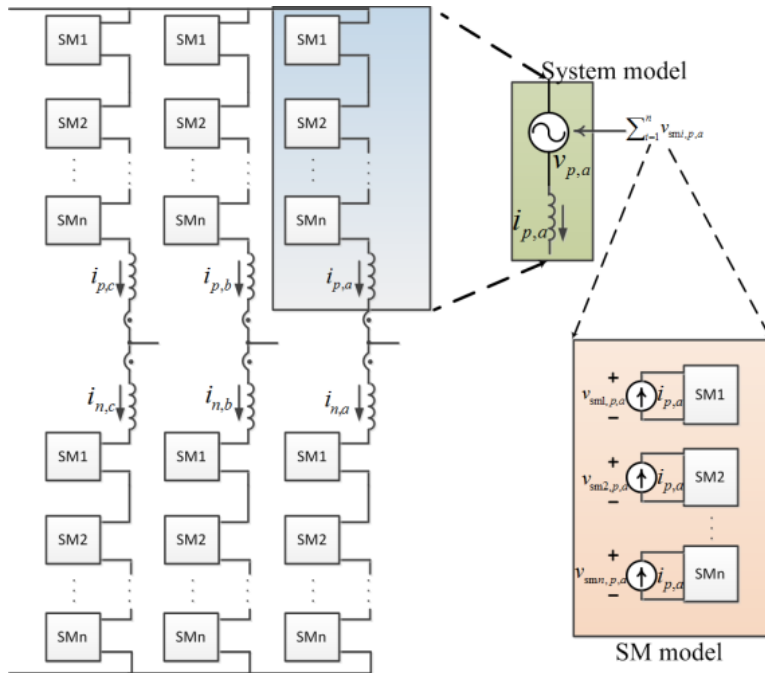


Figure 16: Numerical stiffness based separation of modular multilevel converter (MMC) voltage source converter (VSC) dynamic simulation algorithm

## 2.4 Multi-terminal VSC-HVDC control approach

An example multi-terminal MMC-HVDC system connected to three AC grids is shown in Figure 17. The MMC-HVDC links connected to the AC grids provide inertial support based on the proposed control approach. Some of the events considered to impact frequency include changes in the power processed by the MMCs in a weak grid, loss of generator(s) in the AC grid, loss of loads, and others. The proposed control approach provides the primary response to the frequency events that have occurred. The relocation of power resources between the AC grids, or the secondary response to the frequency events, is implemented by the central energy management system (EMS). The central EMS also sends power dispatch commands based on load-generation forecasting and economics.

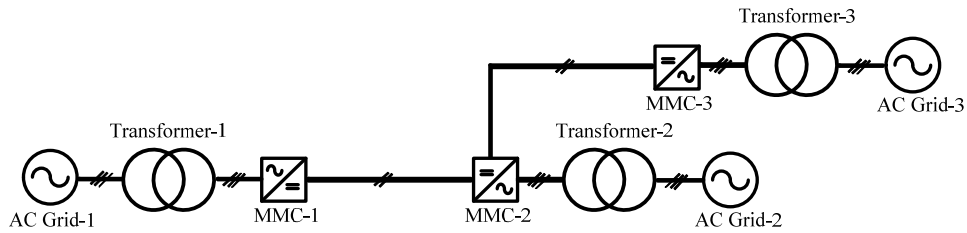


Figure 17: Multi-terminal MMC-HVDC system.

In the proposed control approach, each MMC behaves like an agent in a multi-agent control implementation. In each agent, the following layers of control are present: (i) inner-loop to control AC grid currents, DC-link currents, circulating currents, and capacitor voltages; (ii) outer-loop to control AC frequency, DC voltage control, and active power; (iii) SM capacitor voltage balancing; and (iv) modulation. The inner-loop control system and SM capacitor voltage balancing algorithm are explained in Appendix A.2. The modulation strategy is based on the nearest-level control [Debnath 2015].

### 2.4.1 Outer-loop control system

The AC-side frequency is estimated based on digital implementation of synchronous reference frame phase-locked loop (SRF-PLL) [Golestan 2017]. The SRF-PLL uses the measured AC-side voltage as input.

The expert systems vary the average capacitor voltage and active power during frequency incursions to provide inertial and governor response (like generators). While the variation in the average capacitor voltage is effected during changes in commanded power, the active power is varied during significant frequency events like loss of generators or loads. The frequency disruption observed during change in commanded power is particular noticeable in a weak grid.

The expert system developed to provide the inertial support using the average capacitor voltage is shown in Figure 18. If the estimated frequency is greater than the dead-band setting and there was a change in the commanded power from the central EMS, the average capacitor voltage reference is varied based on the estimated frequency. That is, if the estimated frequency is less than the nominal frequency, energy is supplied to the AC grid and vice-versa. This strategy does not impact the power flow in the DC terminals. The aforementioned thresholds determine the dead-band used on the estimated frequency to avoid spurious events' detection. The aforementioned energy support is of particular importance when there is a change in the commanded power.

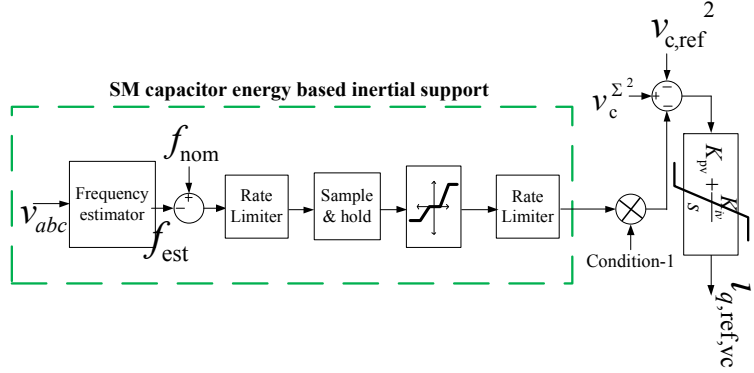


Figure 18: SM capacitor energy based inertial support to weak AC grids.

In the dead-band, the SM capacitor voltages are varied to improve the efficiency of the system through reduction in switching frequency. The corresponding SM capacitor voltage balancing strategy used to maintain the SM capacitor voltages across all operating conditions is explained in detail in Appendix A.2.

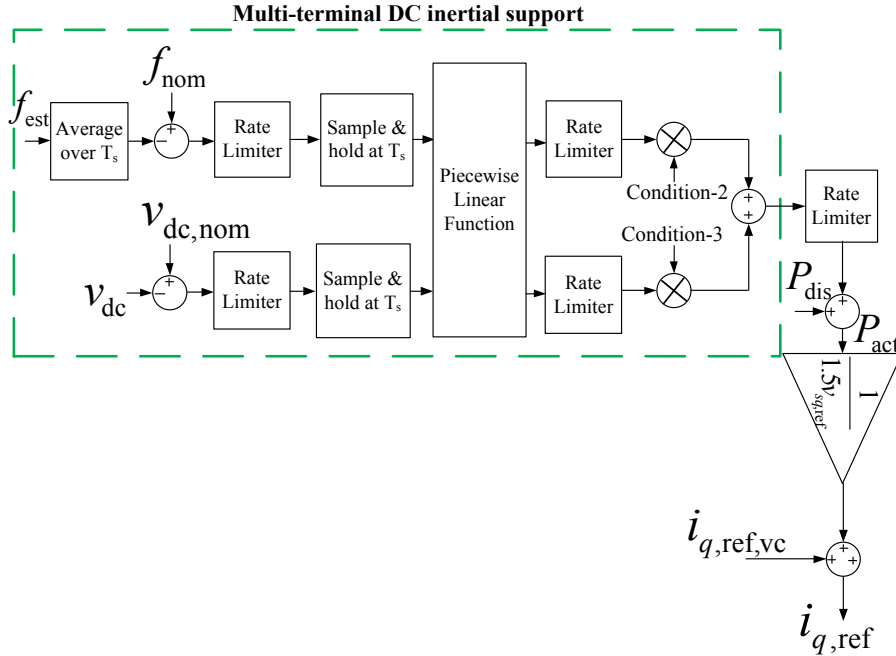


Figure 19: Active power based inertial support.

Based on a dead-band setting on the estimated frequency and if there is no change in the commanded power, the loss of generator or load is assumed. In this scenario, the q-axis AC-side current reference is added to another component based on the change in the frequency. Similarly, the reference to the 0-component of the circulating current is varied based on the estimated frequency to maintain net-zero power between the AC and DC sides. Because the MMC is connected in a multi-terminal configuration, the change in power reference at only one MMC terminal will impact the DC-link voltage. To maintain the stability of the DC system, the other MMCs have to react to the change in power at one of the MMC terminals. Therefore, there is a provision to detect the loss of generators or loads in the AC grid connected to the other MMC terminals through the DC-link voltage. Based on a dead-band setting on the DC-link voltage and if the connected AC grid's frequency is within the dead-band settings, the q-axis AC-side

current and 0-component of the circulating current are varied based on the measured DC-link voltage. If both the DC-link voltage and the connected AC grid's frequency is beyond their respective dead-band settings, then the q-axis AC-side current and the 0-component of the circulating current are varied based on both the measured DC-link voltage and estimated AC-side frequency. The control system to provide inertial support using the active power is summarized in Figure 19. The overall control strategy is summarized in

Figure 20.

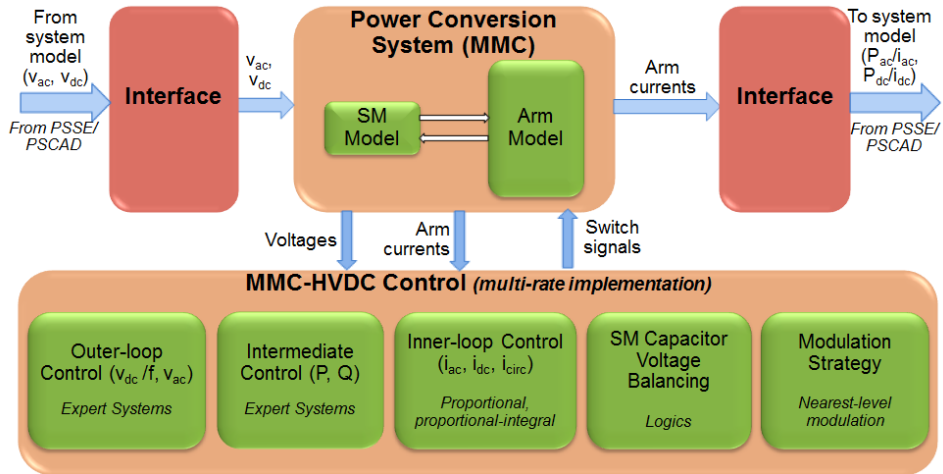


Figure 20: Summary of overall control strategy.



## 3.0 Technical results summary

This section summarizes the technical results from the application of the technical approach from Section 2.0 for the continental-level model, and the high fidelity models.

### 3.1 Accomplishments for power flow and transient stability models with the continental-level model

Power flow and transient stability models for WI and EI were put together and connected through HVDC macrogrid model. These models were used to study provision of congestion relief and frequency/inertial response across both large scale interconnections. This section provides a summary of the resulting large-scale model, which is unique in its size, and the main results of using this model for providing services with HVDC, that are additional to the bulk power transfers.

#### 3.1.1 Model building

Two transfer scenarios were built in this study:

- *Case WECC2EI*: Eastern Interconnection (EI) is peaking and the Western Interconnection (WECC) is supplying 14.4 GW (from otherwise unused capacity)
- *Case EI2WECC*: WECC is at its peak and the EI is supplying 14.4 GW of load diversity capacity to the west

The HVDC macrogrid was designed to transport 14.4 GW power. It consists of 14,  $\pm 800$  kV, 5400 MW links (16,200 MW in total) to allow for frequency response and other reserves.

Given the complexity and the scale of the model to be built, it was decided that widely used HVDC power flow and quasi-steady-state (QSS) dynamic models for planning studies will be employed. The HVDC macrogrid was assumed to be a collection of well tested line commutated converter (LCC) line models.

The AC Interconnection of WECC was represented by a 2025 heavy-summer (HS) planning case provided by WECC; the Eastern Interconnection was represented by 2026 summer-peak model, provided by the Multi-Regional Modeling Working Group of the Eastern Interconnection Reliability Assessment Group (ERAG-MMWG).

The generation was adjusted as the sink and the load as a source in the AC Interconnection-wide WECC and EI power flow models to deliver power through the HVDC macrogrid in the following manner:

- WECC2EI case:
  - WECC in high summer peak conditions had load reduced by 14 GW to model a slightly off-peak loading condition.
  - EI: 14 GW of peaking generation was turned off.
- EI2WECC case:

- WECC: 14 GW of peaking generation was turned off.
- EI generation was the same as high summer peak case, and load was reduced by 14 GW.

### 3.1.1.1 HVDC macrogrid model

Each HVDC link was modeled using the two-terminal DC line model CDC6 in PSS®E. The configuration of each HVDC link as modeled is shown in

Figure 21. A one-line diagram of the developed macrogrid in PSS®E is shown in Figure 22.

Model parameters were set in accordance with typical HVDC models. The power flow model parameters and assumptions were tested using an initial test system with all HVDC links with injections and absorptions by positive and negative loads as a first approximation. After the initial tests were satisfactory, the HVDC macrogrid was incorporated in the full models with EI and WI complete models. The initial tests showed that HVDC model parameters calculated were reasonable, and 8% overall power delivery loss was achieved. The reactive power consumption at converter terminals was around 55% for heavily loaded lines, and firing angles were within the normal operating ranges.

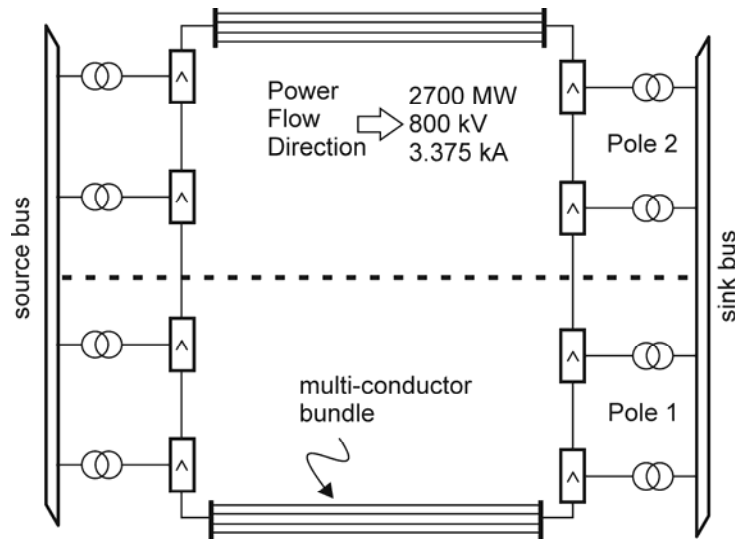


Figure 21: HVDC link configuration

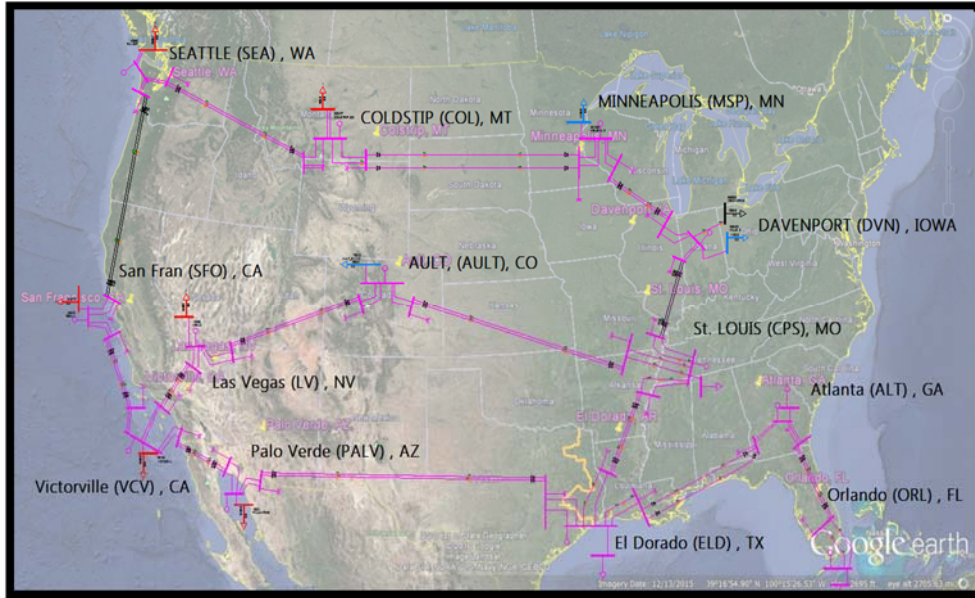


Figure 22: One-line diagram of the HVDC macrogrid

### 3.1.1.2 Combined continental-level power-flow model of WECC and EI interconnections with HVDC Macrogrid

A combined power-flow model representing WECC, EI with the overlay of HVDC macrogrid was developed. Key parameters of the power flow model are shown in Table 1.

Table 1: Case summary of the developed continental-level power flow model

Total Generation	891.1 GW
Total Load	860 GW
Total Reactive Support	173.5 GVA <sub>r</sub>
Number of Buses	100222
Number of AC Branches	126468
Number of DC Lines	74
Number of Generators	13377
Number of Load	60087
Number of Areas	154
Number of Reactive devices	13841

### 3.1.1.3 Locating and sizing synchronous condensers

HVDC installations based on LCC technology require that the AC system has certain short-circuit strength. A technique for calculating effective short circuit strength known as multi-infeed effective short circuit ratio (MIESCR), as described in [Cigre 2008] was followed. At first, short circuit level at all the HVDC point of interconnections (POI) using a WECC+EI combined model was calculated. All loads represented by ZIP model and unsaturated generator source impedances used to calculate the short circuit

MVA. A MIESCR of 3.0 at each POI was considered as a minimum threshold for effective operation of HVDC. Calculations showed that five HVDC POI had MIESCR lower than 3.0, which was consistent with issues seen during model initialization (see Table 2).

Table 2: Multi-infeed effective short circuit ratio (MIESCR)

HVDC Link From	Reactive Power Requirement (Mvar)	SCL (MVA)	Pdctotal	MIESCR	SCL for Target MIESCR =3
ORL					
ALT	504	29418	3930	7.357	12295
MSP	2009	13673	7082	1.647	23255
DVN	0	12163	2693	4.517	8078
CPS	489	9431	5400	1.656	16690
ELD	2523	24087	8445	2.554	27857
PALV	4579	43854	7108	5.526	25902
VCV	2137	27755	7263	3.527	23925
SFO	1660	33922	2905	11.104	10376
VCV	2314	27755	7263	3.503	24103
LV	3257	29460	6297	4.161	22146
AULT	4310	8493	8243	0.508	29037
SFO	689	33922	2905	11.438	9405
SEA	3136	23822	4225	4.896	15812
COL	4127	5559	7746	0.185	27366

To solve the short circuit strength problem, the solution implemented consisted of installing synchronous condensers, where required, to be placed at HVDC point of interconnections. A study was performed to find out the size of synchronous condensers, which provided enough short circuit strength such that MIESCR is greater than 3.0. The chart of Figure 23 shows the results of the sensitivity analysis. Red dot shows the minimum value of short-circuit strength (thus synchronous condenser size) required at each location for the MIESCR threshold of 3. Only those locations where the red dot is lesser than the first blue bar, require synchronous condenser.

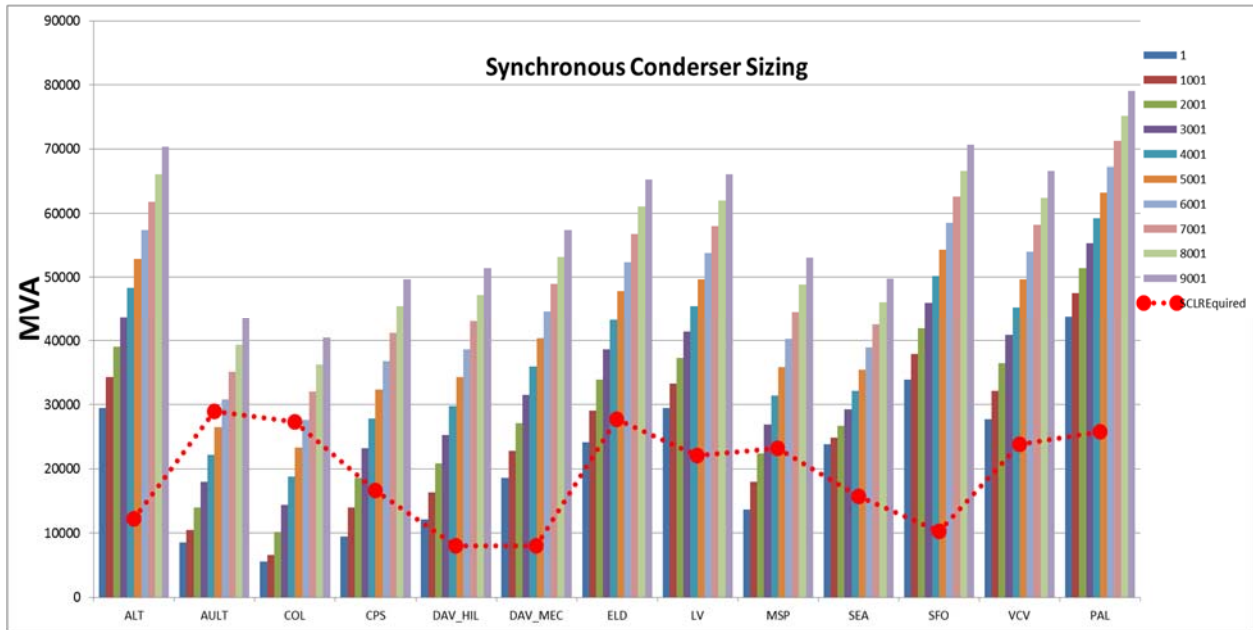


Figure 23: Synchronous condenser sizing to support reactive power consumption of HVDC LCC terminals

The HVDC macrogrid model was subsequently updated with synchronous condensers and successful initialization of combined model was achieved. Any modeling errors and issues were resolved and sanity checks were performed. A 20-second no disturbance, flat start was obtained and some critical disturbances were run on WECC and EI footprint. Results showed expected behavior of the model. A comparison was done with a WECC and EI combined model with HVDC modeled as loads (no physical electrical connections) and WECC and EI with HVDC macrogrid. In a WECC and EI joint model with HVDC macrogrid, if any major unit is tripped on the either side, it also impacts slightly the other side as side because the two interconnections are connected via HVDC macrogrid. Tripping Palo Verde (both units) impacts WECC rotor angles slightly and creates a small drift in relative rotor angles in the EI, as expected.

### 3.1.1.4 Combined continental-level transient stability modeling

A combined dynamic model was developed representing the WECC and the EI with the overlay of HVDC macrogrid. Key parameters of the dynamic model are provided in Table 3.

Table 3: Case summary of the developed macrogrid transient stability model

Model Type	Total number of models
Generator	10631
Exciter	9054
Compensator	1584
Turbine Governor	7242
Power System Stabilizer	3386
HVDC model (LCC, VSC)	45
Wind (with all components)	753
Other User model	3645
WECC CIMWBL	6005
Relay Model	1604

The dynamic models for the Western Interconnection used by industry and provided by WECC were used to represent the WECC Interconnection. Because of the PSS@E memory table limitations, induction motor (CIMWBL) and ZIP load models were used instead of the original, much more complex WECC composite load models. Through the base-case benchmarking studies, the load models were found to be adequate for system frequency response simulation, which is the objective of this project in its first year.

Similarly, the dynamic models provided by ERAG-MMWG were used to represent the Eastern Interconnection dynamic model. Changes to governor models were performed in EI dynamic model data. The reason for improving these models was that original EI dynamic data is very optimistic and does not capture actual system response, as shown in the

Figure 24. Governor model improvements were performed based on an ORNL study [Kou 2014] recommendation. MISO focused on the top three types of governor models used in EI model, and the corrected model performed as shown in Figure 25.

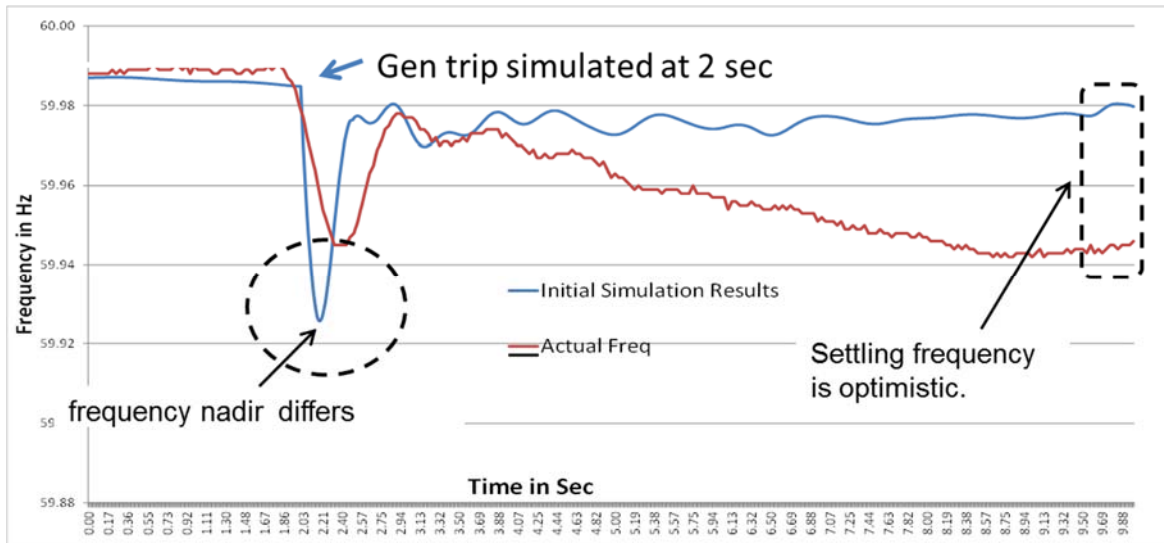


Figure 24 MISO model validation result for Fermi Plant trip

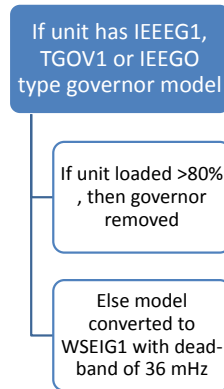


Figure 25 Governor model improvement methodology in EI

The HVDC links in the HVDC macrogrid were represented by the CDC6T HVDC model in PSS®E. The CDC6T HVDC model is recommended for studying new proposed DC lines [Siemens PTI 2013]. Typical dynamic model parameters were provided by Siemens PTI.

Finally, the combined dynamic model was adjusted and issues were resolved to obtain flat voltage and angle plots for a no-disturbance 20-second run.

### 3.1.2 Congestion relief

This study used two types of simulations to show use of HVDC macrogrid to mitigate loop flows and congestion relief: a) a sensitivity study for 2000 MW transfer in EI, and b) congestion relief by making smaller changes in HVDC schedules in the WECC. Figure 26 shows a diagram of the transfers studied in the Eastern and Western Interconnections.

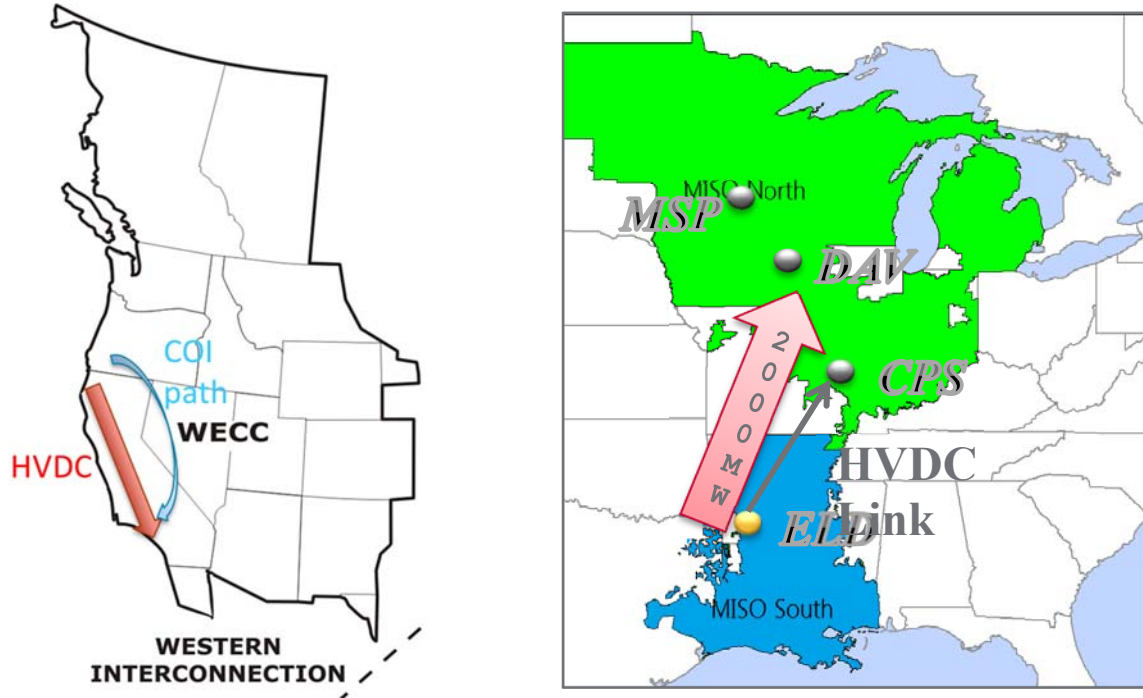


Figure 26: Diagram of transfers analyzed for studying congestion relief in WI (left) and EI (right)

First, three power flow cases were used, in the sensitivity study, in two regions of the EI:

- Case 1: An initial base case to provide a reference and seed
- Case 2: An increase of 2000-MW transfer from the south region to north region through scaling load and re-dispatch of generators
- Case 3: 2000-MW power transfer through an HVDC line.

The sensitivity of these lines was calculated by examining the differences in flow of the transmission lines in each case compared to that of the base transfer case, based on the following equation. The results are shown in Figure 27. It should be noted that the lines with a higher sensitivity in Case 3 are likely because they are close to the HVDC terminals. The flow would occur as a result of HVDC schedules.

$$sensitivity = \frac{|Line\ Flow\ Case(n) - Line\ Flow\ Case\ 1|}{Transfer\ Flow}$$

Using the HVDC macrogrid in the EI could have several benefits: 1) Negate flow in New Madrid transformers (PTDF: without HVDC, it is 13.3% and drops to 1.6% with HVDC); 2) Lower impact on high AC PTDF lines; 3) Selected NERC flow rates have improved PTDFs.

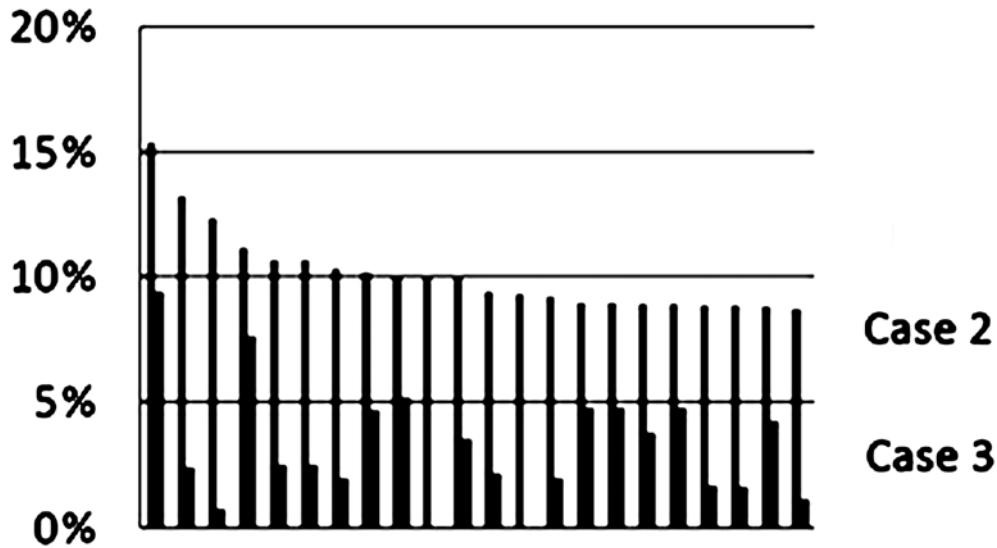


Figure 27: Line sensitivities

Second, to study congestion relief in the WECC, power transfer distribution factors (PTDF) with respect to HVDC injections were used in this study. The EI2WECC case was used, with the sink/source (or buyer/seller) set as either side of the HVDC interconnection. The flow studied was the HVDC macrogrid from the Seattle to San Francisco POIs. A change in 1 MW of the HVDC schedule helps alleviate 0.5 MW on COI path. Additionally, Figure 28 shows the PTDF of each monitored flow path within WECC, with the y-axis as the actual flow, to give it some perspective.

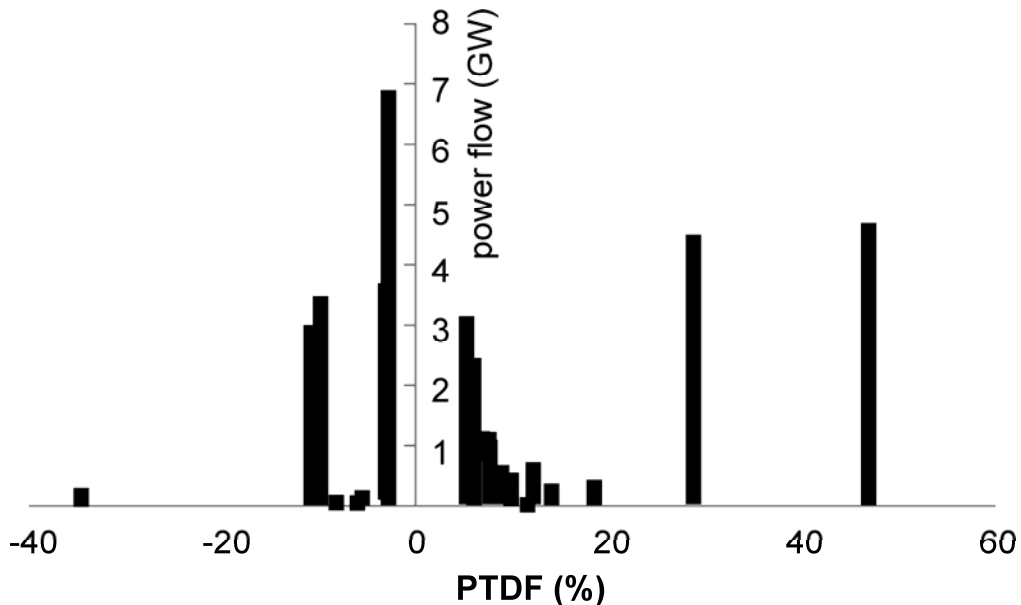


Figure 28: The PTDFs of studied paths within WECC

### 3.1.3 Frequency and inertial response

This section provides results for both the localized and centralized frequency and inertial response provision by the HVDC macrogrid.

### 3.1.3.1 Results for localized control

First, for the localized control strategy, a contingency of loss of two largest generation units (about 2700 MW in total) in WECC system was simulated for 2.0 seconds. The responses of the three HVDC lines to the contingency are shown in Figure 29. The contingency caused frequency drops at the AC stations on the WECC side of the three HVDC systems. Consequently, the localized frequency auxiliary controllers responded to the frequency deviation and automatically changed the HVDC power schedules. The maximum additional power support from the EI system to the WECC is about 1000 MW for the generation loss of 2700 MW in WECC system. As the governors in the WECC system started to respond and system frequency gradually recovered, the auxiliary power from HVDC lines decreased. This showed the advantage of the localized control in terms of adapting to the system conditions.

Figure 30 shows that with the frequency control responses from the HVDC lines, the frequency nadir point in the WECC system is increased by 0.05 Hz (50 mHz), which is corresponding to about 33% improvement in term of the frequency drop magnitude. Damping in the WECC system is also improved. For the EI system, the overall impact is marginal and the frequency nadir point is about 59.965 Hz.

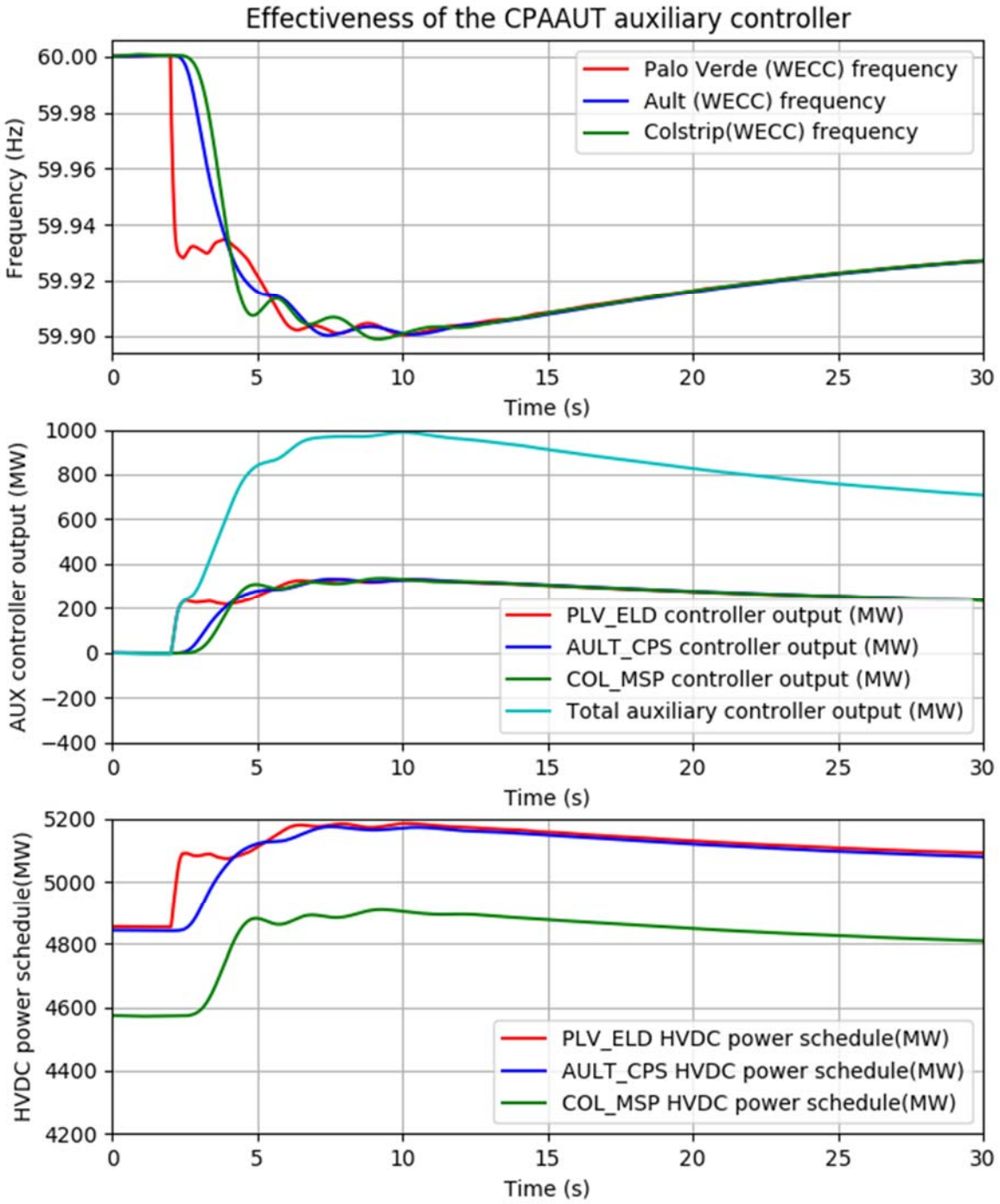


Figure 29: Responses of the three HVDC lines with the CPAAUT auxiliary signal controller

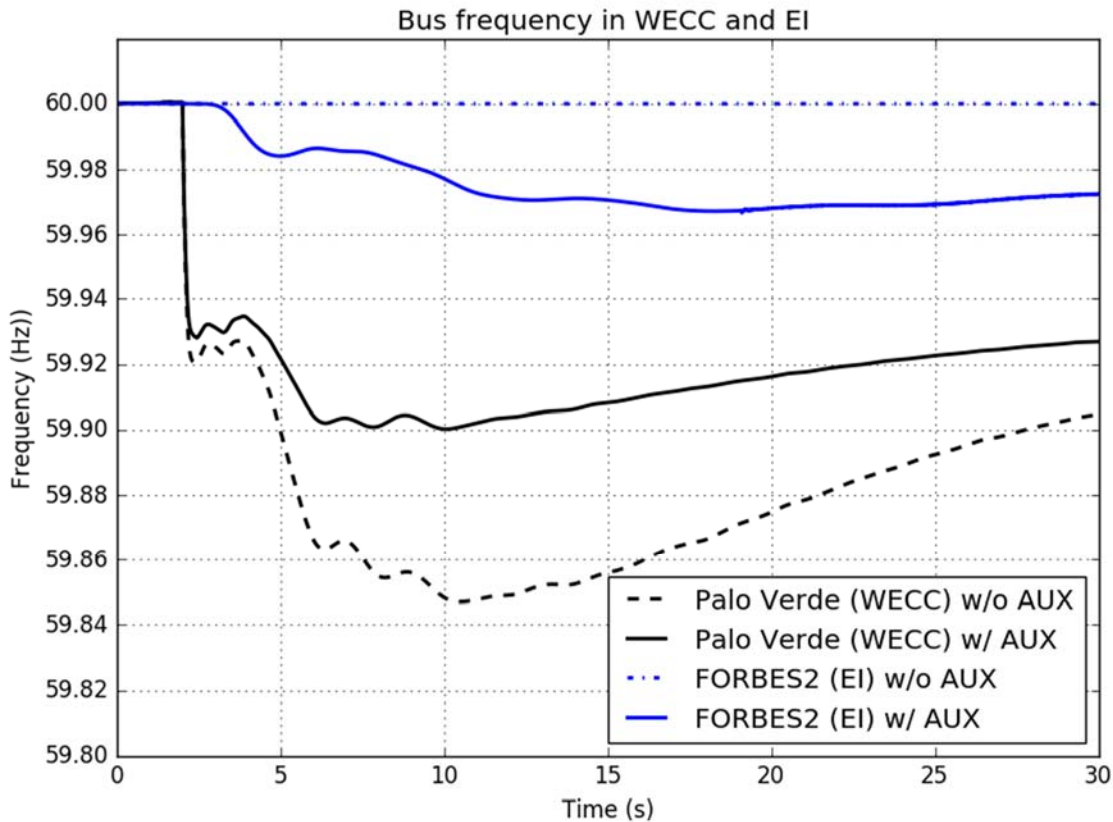


Figure 30: Comparison of the frequency responses for the scenarios with and without the HVDC frequency auxiliary controllers.

### 3.1.3.2 Results for centralized control

This section shows results of the conceptual centralized control proposed in this work.

Three scenarios were studied: 1) tripping of Fermi nuclear plant located in Michigan (EI), 2) tripping of Grand Gulf nuclear plant located in Mississippi (EI), and 3) 2 units of Palo Verde nuclear plant tripping in Arizona (WECC).

The loss of generator(s) was simulated at 0.5 seconds and the simulation was allowed to run for next 2 seconds. A time lag of 2 seconds is assumed to account for data latency, time required for the central controller for event detection and calculating new schedules and each HVDC link receiving new schedules from the controller. The HVDC links are ramped up to the new schedule in the next 1 second and the simulation is run for a total of 20 seconds. Sensitivity scenarios were performed by slowing down the ramp rate of HVDC to 2 seconds. When performing Fermi nuclear plant trip analysis, the schedules of three HVDC links going east to west were changed. For Grand Gulf trip, schedules of major east to west links along with Minneapolis (MSP) to Davenport (DVN) and El-Dorado (ELD) to St. Louis (CPS) were adjusted.

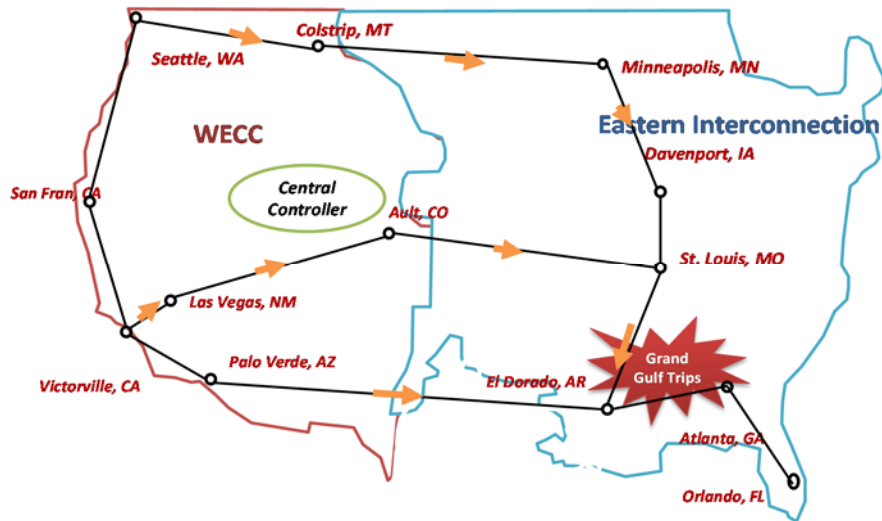


Figure 31: HVDC schedule changes for Grand Gulf trip

For simulating Palo Verde trip, the schedules of the HVDC links, which were changed, are shown in Figure 32. The direction of arrows shows the direction of change in HVDC schedule. For example, in the base case, the San Francisco (SFO) to Victorville (VCV) HVDC link is transferring energy from VCV to SFO (northward). During the simulation, the SFO-VCV HVDC schedule is decreased and the HVDC schedule from the VCV to Palo Verde (PLV) link is increased. This ensures there is minimal impact on the underlying AC system and provides the frequency support in the disturbed area.

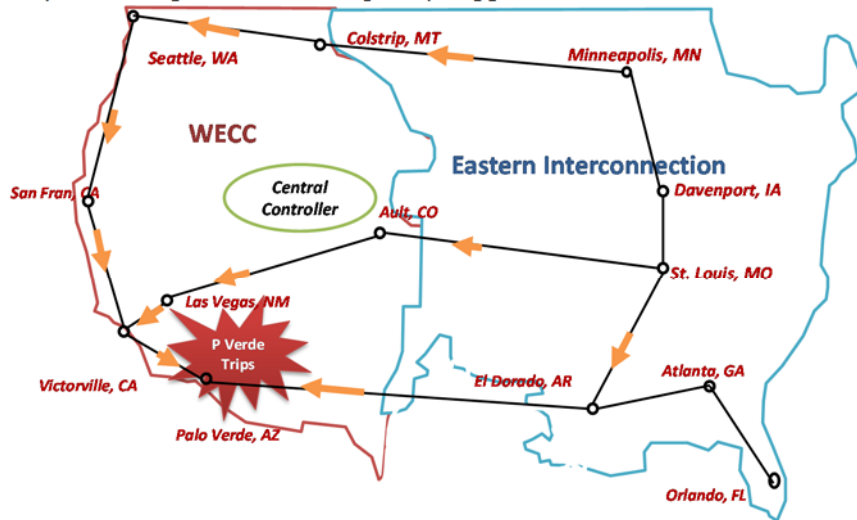


Figure 32 HVDC schedule changes for Palo Verde trip

Simulation results for Fermi nuclear plant is shown in the Figure 33. The blue trace shows the frequency response at a 345-kV network bus near the Fermi unit in the base case. The corresponding value of HVDC schedule of PLV-ELD link is shown by black trace, which remains unchanged, demonstrating no frequency support from the HVDC macrogrid. The green and the pink traces shown the frequency at the same 345-kV bus when HVDC macrogrid supports frequency response with two different ramp rates. It can be observed that HVDC macrogrid successfully provides frequency support in EI, and there is a considerable improvement in the settling frequency at the end of simulation.

The simulation result for the Grand Gulf unit trip is shown in Figure 34. It can be observed that system frequency settles at a higher value, demonstrating successful HVDC frequency response support from the HVDC macrogrid.

The simulation results for Palo Verde Unit 1 and 2 trips are shown in Figure 35. Similar results are obtained; HVDC macrogrid provides considerable improvement in frequency response in WECC. Frequency response of EI is also plotted and provides useful insight on the impact on the frequency behavior of the EI, which is supporting WECC in this scenario. No issue is observed in the frequency response of the EI.

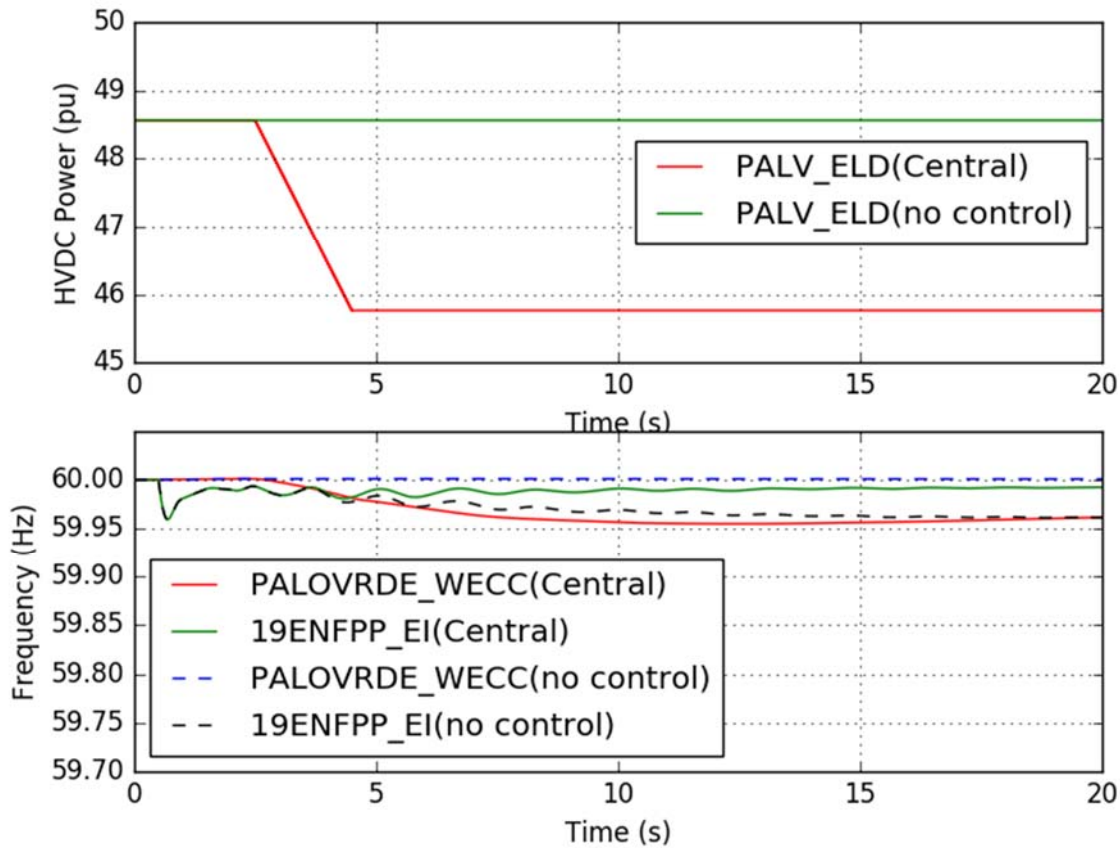


Figure 33: HVDC frequency response for Fermi trip

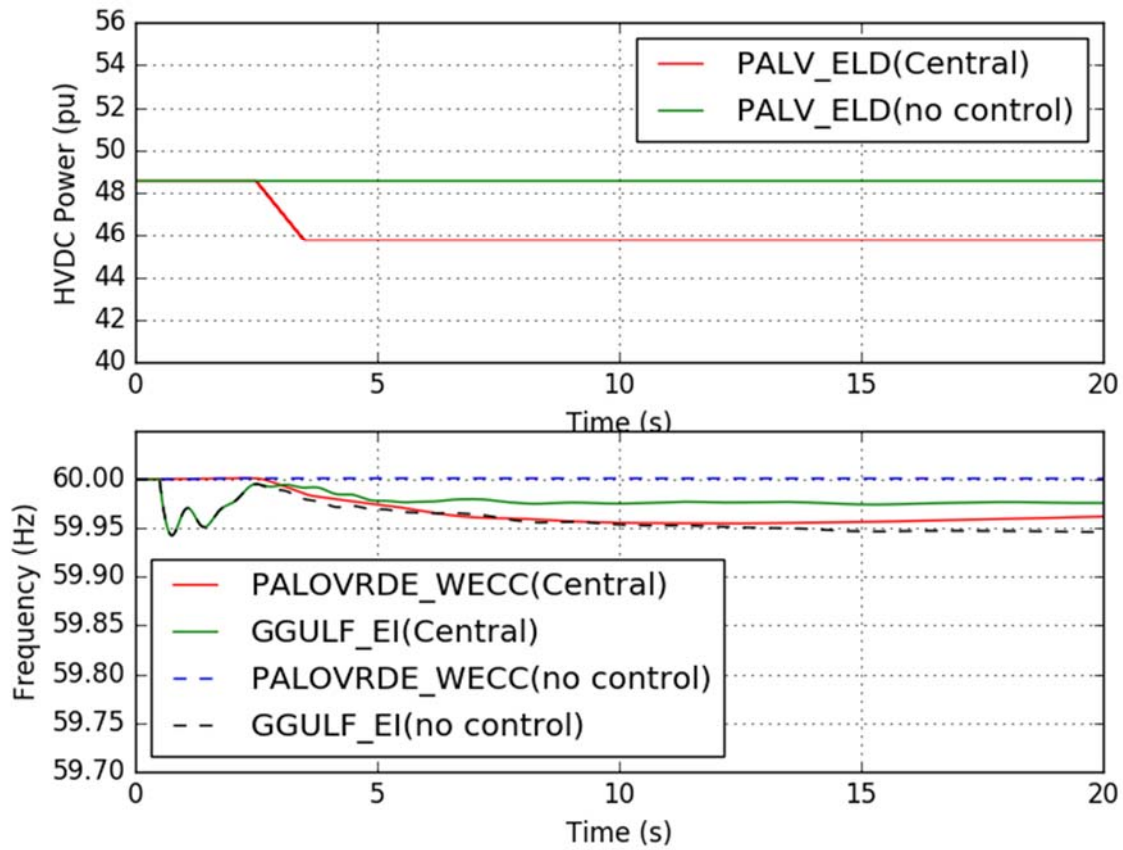


Figure 34: HVDC frequency response for Grand Gulf trip

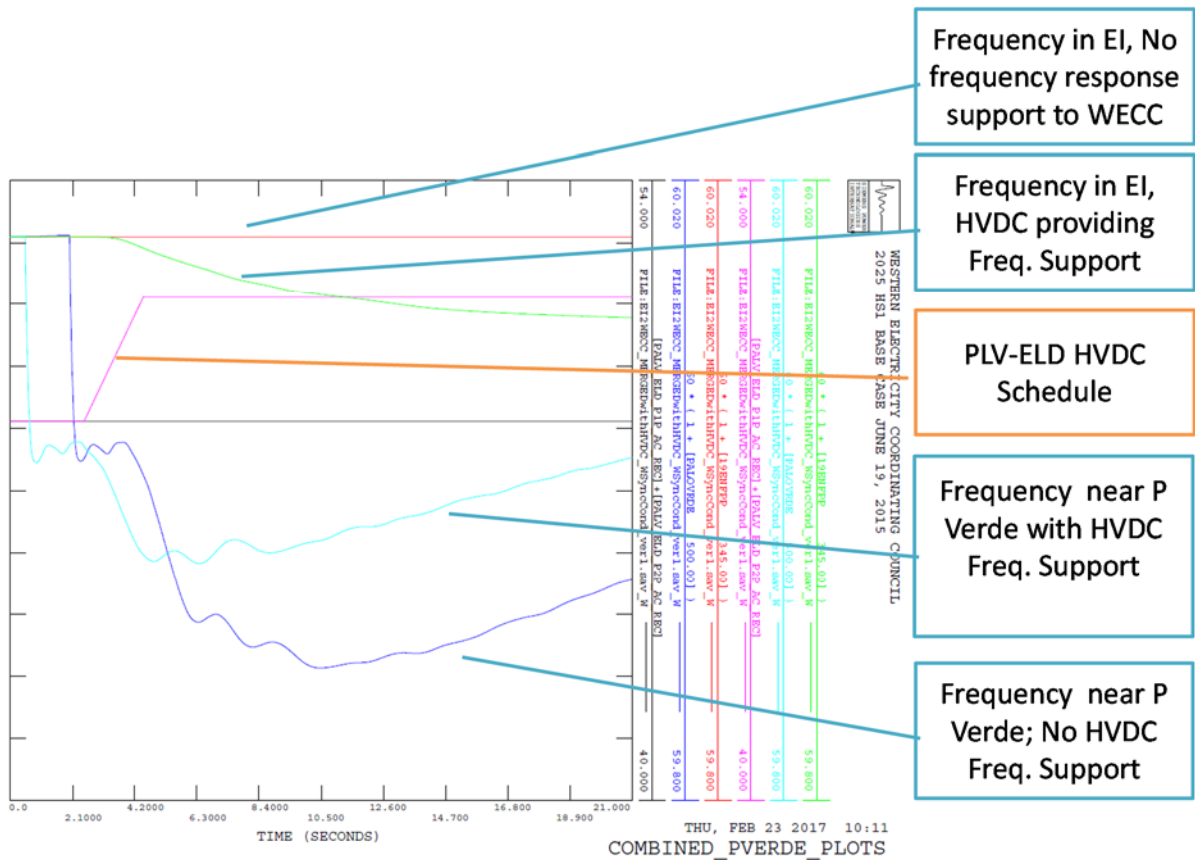


Figure 35: HVDC frequency response for Palo Verde both units trip

For the Palo Verde trip, the impact on NERC’s frequency response measurement (FRM) [BAL-003-1 2008] was calculated, and the results are shown in Table 4. The centralized controller yields 46% higher FRM than the situation without controller. This is because the central controller provides a sustained HVDC response between 20-52 seconds, which is critical for measuring the frequency response obligation per [BAL-003-1 2008]. The central controllers can also be utilized to optimize the HVDC schedule for steady-state power transfer. Future research may include designing a control scheme that combines the central controller with localized faster controllers.

Table 4: Results of frequency response measurement for central controller

	Central Controller	W/out Controller
Gen Loss (MW)	2700	2700
fa (Hz)	60	60
fb (Hz)	59.937	59.90
FRM (MW/Hz)	<b>4383.35</b>	<b>2994.1</b>

## 3.2 Results from high-fidelity modeling and multi-terminal approach

### 3.2.1 Validation & comparison of proposed MMC model

A comparison of the proposed MMC model under the worst-case scenario with the existing models [Gnanarathna 2011, Saad 2014] in the best-case scenario shows a six times fewer floating-point operations requirement. Up to 25 times fewer floating-point operations are required with the proposed MMC model compared to the existing models.

A comparison of the proposed MMC model with a detailed reference MMC model developed in PSCAD/EMTDC is performed. The proposed model is developed in FORTRAN90 language and embedded within PSCAD/EMTDC. The detailed reference MMC model is developed based on the basic building blocks in PSCAD/EMTDC like IGBTs, diodes, inductors, and capacitors. The parameters that describe the test MMC system are presented in Table 5. The corresponding simulation parameters are presented in Table 6.

Table 5: MMC system parameters

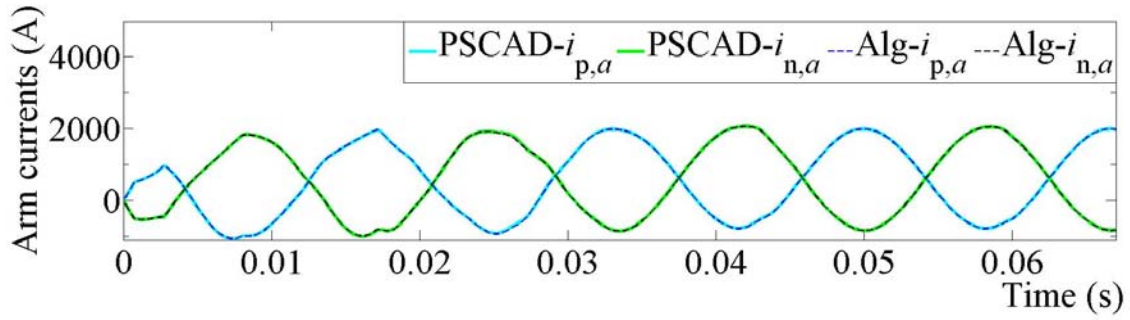
Parameter	Value
<b>N</b>	400
<b>C<sub>sm</sub></b>	15 mF
<b>R<sub>p</sub></b>	20 kΩ
<b>V<sub>dc</sub></b>	400 kV
<b>f</b>	60 Hz
<b>V<sub>s</sub></b>	333 kV (line-to-line, rms)
<b>L<sub>s</sub></b>	80 mH
<b>R<sub>s</sub></b>	0.8333 Ω
<b>L<sub>o</sub></b>	65 mH
<b>R<sub>o</sub></b>	0.1 Ω

Table 6: Simulation parameters

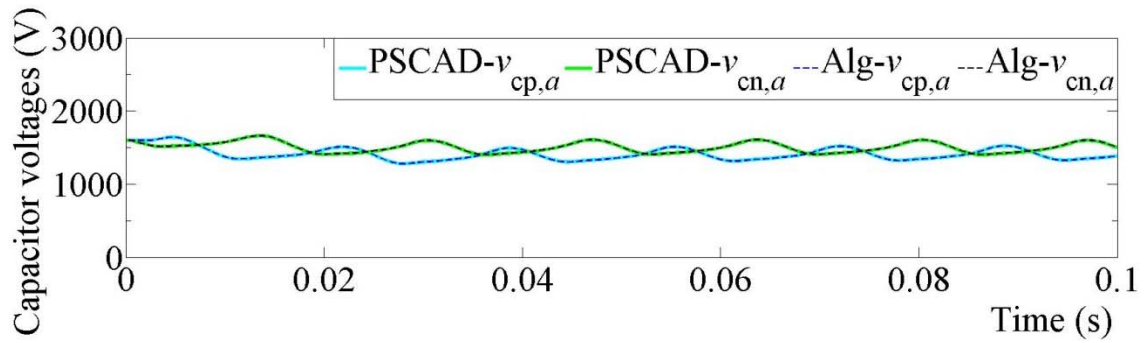
Parameter	Value
<b>h</b>	4 us
<b>R<sub>on</sub></b>	1 mΩ
<b>R<sub>off</sub></b>	1 MΩ

The errors observed between the states of the MMC in the simulation of the proposed MMC and the detailed PSCAD/EMTDC reference MMC models are less than 1%. The states are shown in Figure 36 for visual comparison. The results presented are under steady-state operation of the MMC-HVDC. The states of the MMC under transient conditions and DC faults are shown in Figure 36 and Figure 37, respectively. All the results show very low errors between the proposed MMC model and the detailed

PSCAD/EMTDC reference model. The computational speedup of the proposed algorithm with respect to the reference model is 200,000.

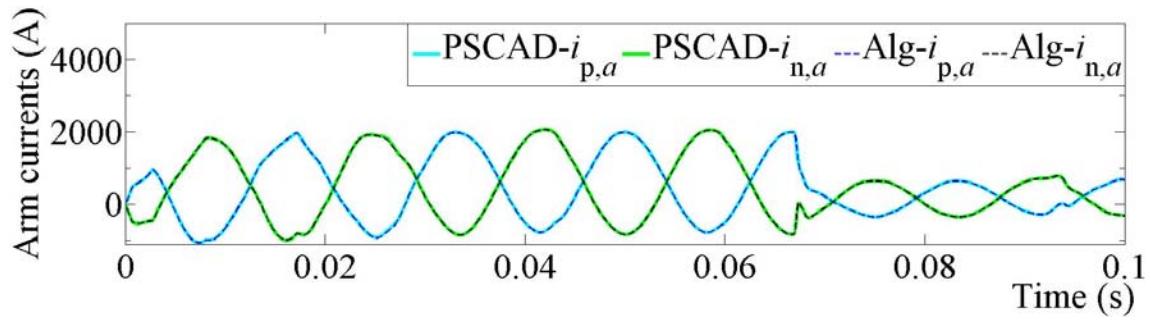


(a)

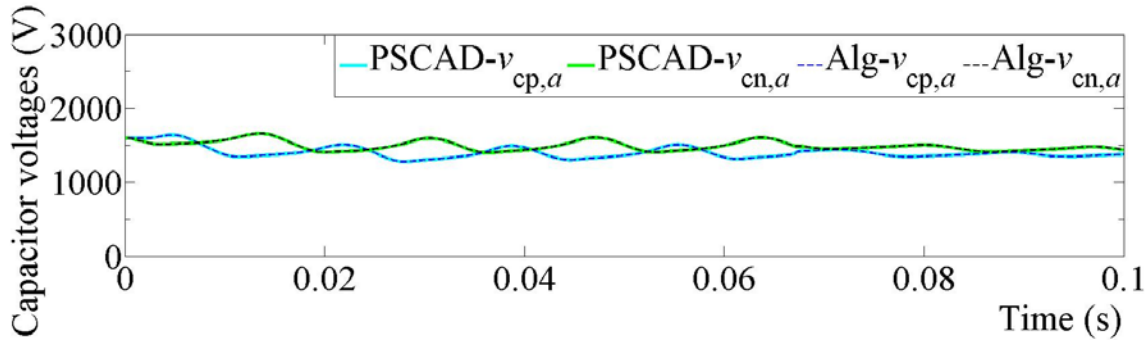


(b)

Figure 36: States of MMC under steady-state: (a) phase-a arm currents, and (b) phase-a average capacitor voltages in each arm



(a)



(b)

Figure 37: States of MMC under steady-state: (a) phase-a arm currents, and (b) phase-a average capacitor voltages in each arm

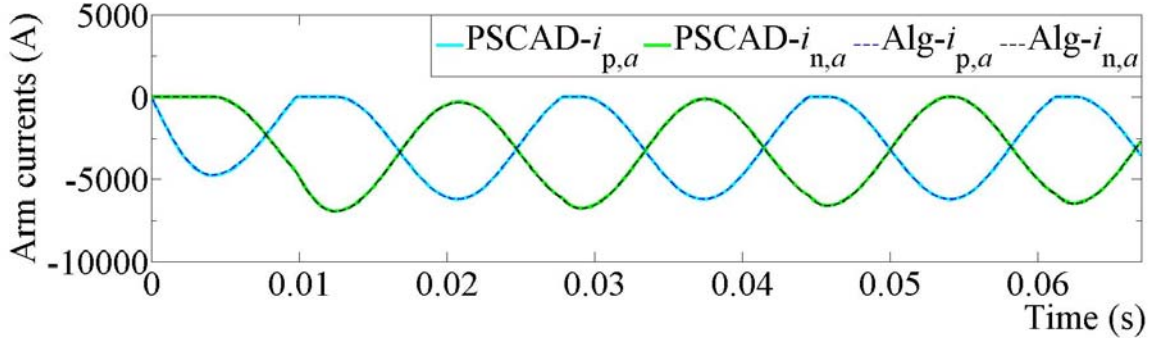


Figure 38: MMC phase-a arm currents under DC fault condition.

### 3.3 Multi-terminal VSC-HVDC across EI-ERCOT-WECC

A multi-terminal VSC-HVDC (MTDC) system connecting EI, Energy Reliability Council of Texas (ERCOT), and WECC is considered to test the developed control strategy. The corresponding system is shown in Figure 39. This case-study assumes single point of injection of the HVDC into each asynchronous interconnection. The AC grids shown in Figure 39 represent the aggregated models for EI, ERCOT, and WECC based on NERC data available [NERC 2011]. While second-order dynamic system models are shown to represent the frequency characteristics of EI and ERCOT, the AC grid model in WECC uses the WSEIG1 model [Kou 2016] to accurately represent the frequency dynamics.

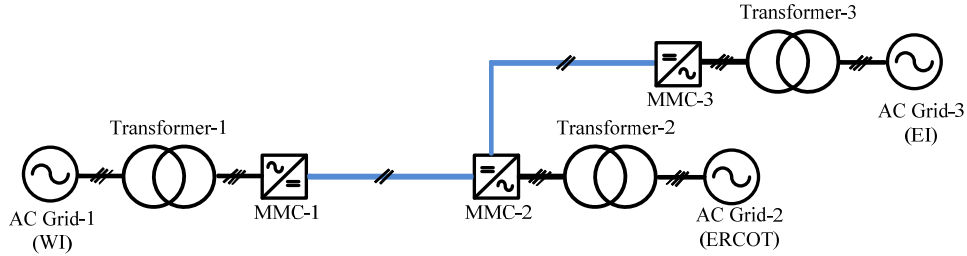
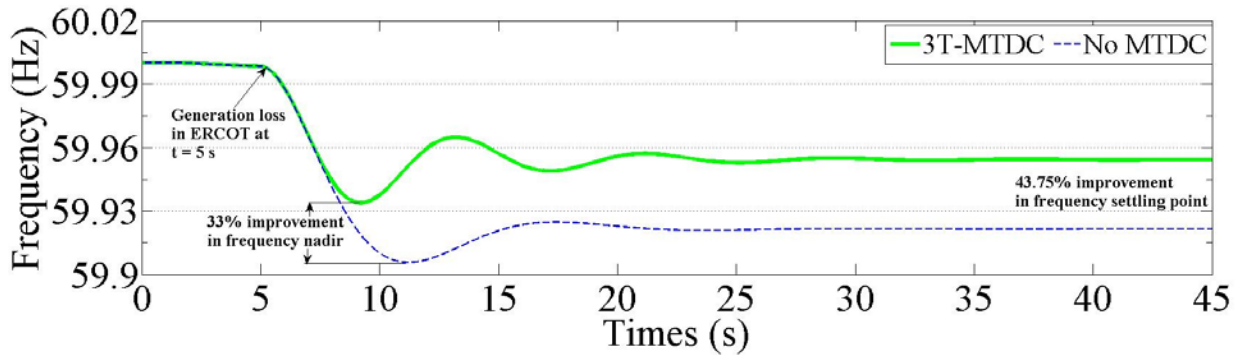
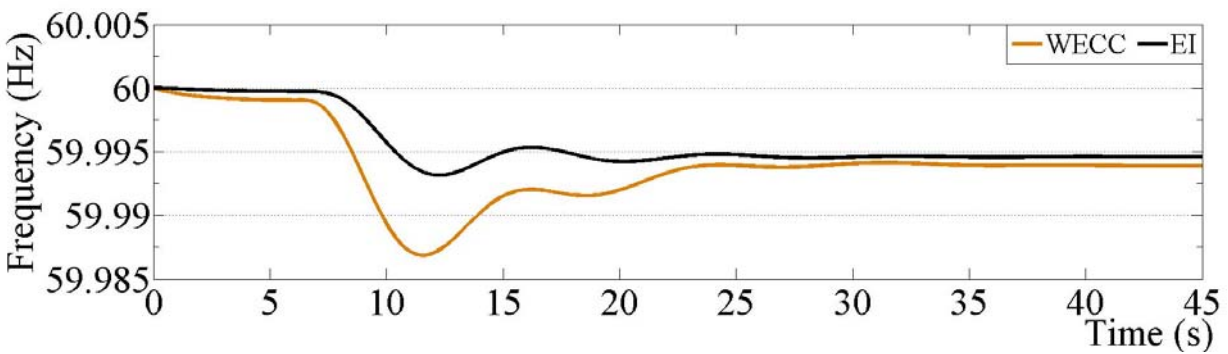


Figure 39: Multi-terminal MMC-HVDC system connecting three asynchronous grids in US.

Three case studies are considered: (i) 500-MW generation loss in ERCOT, (ii) 500-MW generation loss in WECC, and (iii) 1000-MW generation loss in EI. The impact of the corresponding losses is shown in Figure 40, Figure 41, and Figure 42. The presence of the MTDC improves the primary frequency response in each interconnection by between 19 and 44%. The improvement is noticed in the frequency nadir and the frequency settling point. When one interconnection loses generation, the other interconnections' frequency is also impacted because the MTDC enables sharing of the frequency deviations between the interconnections. The aforementioned sharing of frequency can be noticed through the impact on other interconnections in Figure 40 (b), Figure 41 (b), and Figure 42 (b).

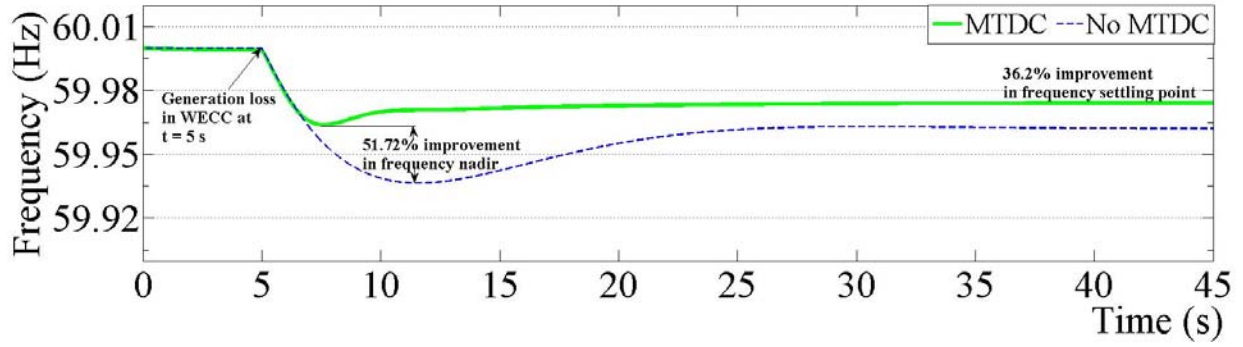


(a)

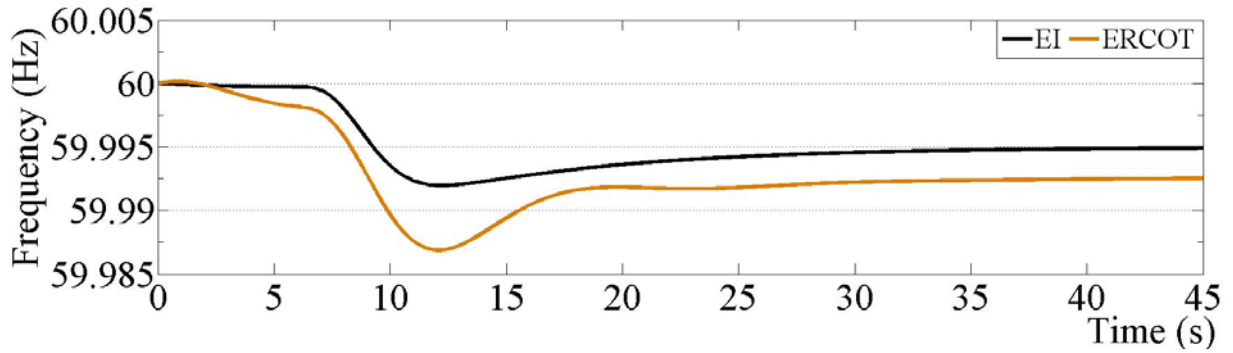


(b)

Figure 40: Frequency response provided by the MTDC system to support 500-MW loss in ERCOT: (a) Comparison of frequency in ERCOT with and without MTDC, (b) Frequency in EI and WECC with the MTDC support to ERCOT.

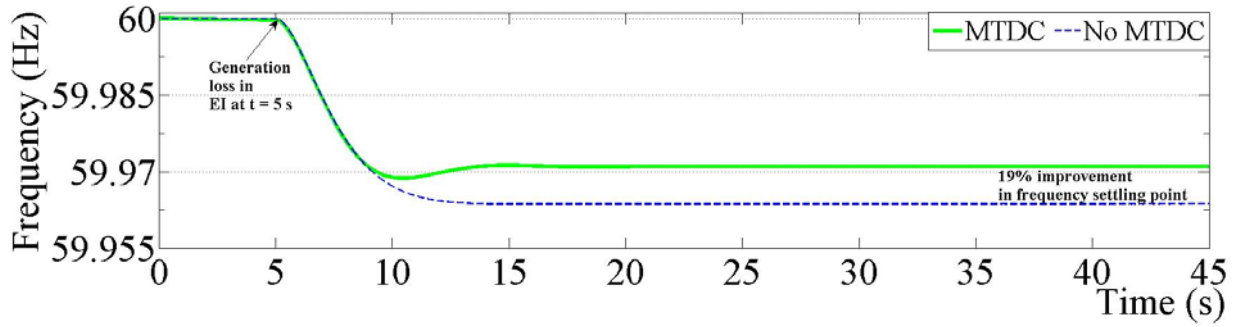


(a)

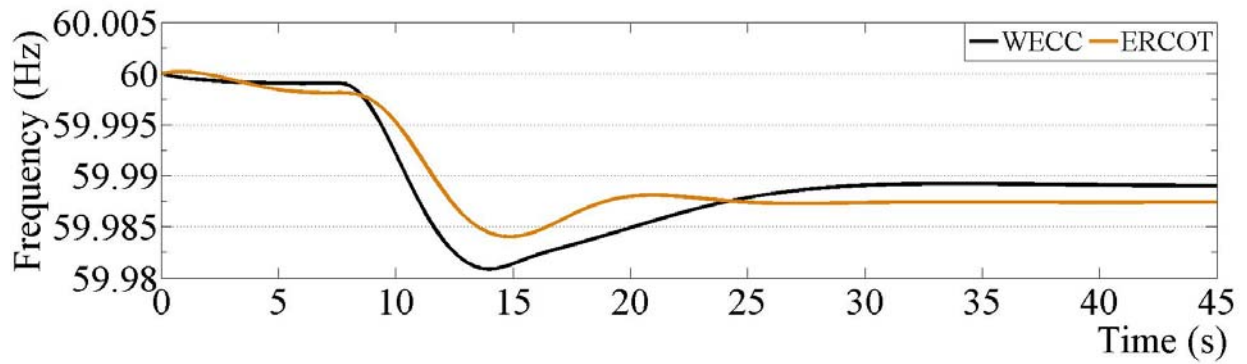


(b)

Figure 41: Frequency response provided by the MTDC system to support 500-MW loss in WECC: (a) Comparison of frequency in WECC with and without MTDC, (b) Frequency in EI and ERCOT with the MTDC support to WECC.



(a)



(b)

Figure 42: Frequency response provided by the MTDC system to support 1000-MW loss in EI: (a) Comparison of frequency in EI with and without MTDC, (b) Frequency in ERCOT and WECC with the MTDC support to EI.

## 4.0 Conclusions, lessons learned, and future work

This project tested initial technical feasibility and showed use of HVDC macrogrid for frequency control and congestion relief in addition to bulk power transfers. The project used both industry-established models for commonly used technologies, and developed high-fidelity models for recently developed HVDC converter technologies, the voltage source converters (VSC) modular multilevel converters (MMCs). The industry-established models were used in large continental-level power system models of the two largest North American interconnections. While the high-fidelity models were developed in detail for HVDC systems in point-to-point configuration and tested in a three-node multi-terminal configuration.

### 4.1 Conclusions

This work developed a continental-level mixed AC-DC grid model of North America using a HVDC macrogrid power flow and transient stability model connecting Eastern Interconnection (EI) and Western Interconnection (WI) models. The HVDC macrogrid is based on commonly used point-to-point line-commutated converter (LCC) DC technology. The developed models use Western Electricity Coordinating Council (WECC) 2025 heavy summer and EI multi-regional modeling working group (MMWG) 2026 summer peak cases. The models showed that the HVDC macrogrid relieved congestion and mitigated loop flows in AC networks, and provided up to 24% improvement in frequency responses. They showed that the current infrastructure can accommodate HVDC injections.

Computational speed of the high-fidelity MMC VSC dynamic models was also an achievement. The models resulted in 200,000 times faster simulation speed when compared to detailed reference PSCAD/EMTDC models. It is also up to 25 times faster than the existing simulation algorithms for MMC VSC systems. The errors in the developed model with respect to the reference models in PSCAD/EMTDC have been shown to be less than 1%. The model developed can be scaled to multi-terminal configurations, which are not available in PSS®E today.

Control algorithms that support smart and autonomous operation of multi-terminal MMC-HVDC systems were developed and tested on a three-terminal case study. The three-terminal case study considered single point of injection of HVDC in to the three asynchronous grids in US: EI, ERCOT, and WECC. These grids were modeled in a simplified way as a first step. The studies showed between 19% and 45% improvement in the frequency nadir and the settling point post generation loss in each interconnection. The project economic savings from frequency sharing between the three interconnections has been shown to be \$5-\$10 billion [MISO 2014].

### 4.2 Lessons learned

This study performed an initial feasibility study of a continental-level interconnected power system employing multiple HVDC lines in macrogrid configuration, interconnecting the Eastern and Western North American power grids. Technical feasibility utilizing industry-grade power flow and dynamic models for large interconnections was shown. A topology much like that proposed in previous work [MISO 2014] was adopted with some changes with total transfers of 14.4 GW between the Eastern and Western Interconnections. From these simulations, the following lessons were learned:

- Currently planned infrastructure can accommodate the HVDC injections.

- Dynamic performance of the continental system is acceptable.
- HVDC macrogrid can be used to improve dynamic performance by adding auxiliary control to some HVDC lines.
- Existing planning tools can be used to conduct initial study.
- Higher detailed models might be needed for some applications; however, a need for more detailed model has not been evaluated for the applications and assumptions studied this year for the full HVDC macrogrid – Eastern – Western interconnected model.
- The HVDC macrogrid was modeled at the continental level based on well-established LCC-based technology, and point-to-point LCC-HVDC systems based on an assumption of ~3-4 GW power transfer approach at some nodes was used. Simulation was performed with readily available industry-accepted models in PSS®E. The advantage of these configurations is that large bulk energy transfers can be achieved with present-day technologies.
- Newer VSC-HVDC systems could introduce additional benefits to AC systems; however, there are some limitations in modeling for large interconnected systems.

A preliminary economic study of a point-to-point LCC layout and a multi-terminal VSC layout in the United States shows higher benefits provided by the VSCs. The corresponding LCC layout and multi-terminal VSC layouts are shown in Figure 43.

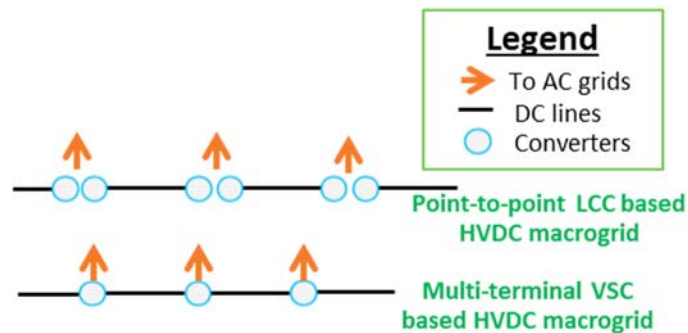


Figure 43: A comparison of point-to-point LCC layout and multi-terminal VSC layout for the macrogrid.

The benefits accrue from the cost, efficiency, and space savings. The data used for this purpose was obtained from [Mukhedkar 2011, Sellick 2012]. The results of the comparison are shown in Table 7.

Table 7: Benefits of VSC over LCC

Quantity	VSC:LCC (Multi-terminal: Point-to-point)
Converters/terminal	1:2
Cost	1:1.74
Efficiency	1:1.2
Space	1:3.44

Other benefits provided by the VSCs (like fast response, voltage support, black-start, and islanded operation) need to be studied to quantify greater economic benefits.

The high-fidelity models developed in this project help with understanding the fast response of the VSCs and the ability of multi-terminal systems to connect to AC grids of varying strengths. The grid strength is quantified by the short-circuit ratio in this case. The grid strength assumes significance to allow integration of stochastically variable renewables.

The high-fidelity models generated require significant computational resources to capture the dynamics of the advanced DC-AC grids of future. They also require hardware data and real-time control hardware to help with the future grid developments.

### 4.3 Future work

Preliminary economic analysis shows a cost ratio of 1:1.74 between point-to-point LCC-DC system and multi-terminal VSC DC system. Despite the cost benefits of multi-terminal VSC-DC systems, LCC-DC systems are still required for bulk power transfers ( $> 4$  GW). Based on the aforementioned benefits of each system, various scenarios and DC systems' penetrations along with economic benefits provided by these systems will be studied in the second year of this project. The project will also model other VSCs to understand feasibility of multiple vendors participating in the future developments. It will also introduce other ancillary services to the multi-objective optimization and control that have not been considered. Additional ancillary services to include could be voltage control, provide dynamic contingency response, damping of oscillations, etc. Economic and reliability benefits derived from these services will also be quantified through understanding enhancements in grid reliability. An industry advisory board (IAB) will assist the National Laboratories with building the accurate realistic cases for simulations.

The reliability and economic assessment will aim at finding benefits of the additional services (such as congestion management, frequency response, contingency response) provided by HVDC systems, other than bulk transfers of energy between regions. The project team will aim at capturing the value of the flexibility and controllability introduced by the DC systems into the AC large interconnections.

The objectives for the second year of this project are highlighted below:

1. Develop and evaluate different scenarios of DC system penetrations in the future grid. This work will facilitate understanding of required grid expansion plans and the potential benefits, and sensitivities to

scenarios of topology and technology. The multi-terminal DC system models created in this project will be used for this purpose.

2. Develop high-fidelity dynamic models of multi-terminal DC systems based on other voltage-source converters (VSCs) like cascaded two-level (CTL) converter and alternate-arm converter (AAC). The developed models will enable planners to make informed choice of the required technology in the future grid expansion.

3. Building up on the three-terminal case-study in this project, feasibility of multi-terminal VSC-DC systems beyond three-terminals to provide multiple injection nodes in each asynchronous grid will be considered. Initial economic assessment has shown the advantages of using multi-terminal systems to LCC systems at 1:1.74. LCC systems will still be required for bulk energy transfers.

4. Include and rank more objectives in the multi-objective DC control algorithms (advanced DC control strategies) such as use of DC system in strategies to mitigate dynamic contingency response in the DC and AC systems, damping of oscillations, voltage control, etc. The economic and reliability benefits associated with such responses and additional services provided by DC systems will be provided.

5. Improve the criteria of selection and placement of the DC technologies based on the aforementioned technical and economic analysis.

6. Disseminate findings of first and second year of this project by organizing industry advisory board meetings and submitting papers to conferences and journals

#### **4.4 Final outcome**

This project will equip decision makers and planners with high-fidelity models that enable analysis of economic benefits of various penetrations of DC in today's AC grid. It will also provide designs of a hybrid LCC-VSC macrogrid connecting the asynchronous interconnections and enabling the introduction of different energy sources like wind, solar, and others. In the hybrid macrogrid, the LCC nodes will be used for bulk transmission and the VSC nodes will be in multi-terminal configuration in the hybrid macrogrid.

#### **4.5 Industry advisory board discussions and feedback**

The project team presented intermediate progress to an industry advisory board (IAB). The IAB assisted the National Laboratories with building the accurate realistic cases for simulations. IAB feedback on scenarios of study, use cases, and events of interest was provided. There were three IAB meetings with participants from the following institutions: CAISO, Xcel Energy, WAPA, SDG&E, BPA, Idaho Power, GaTech, TGS, NREL, SPP, Siemens, MISO, ORNL, and PNNL

The main feedback reviled from the IAB was:

- The meeting were well attended, especially the third meetings, and high interest in industry was perceived.
- Some IAB members showed interest in joining the project team to provide additional feedback and participation.
- IAB members were interested in having access to the models developed in this project.

- Technical feedback from IAB included: consideration of N-1 reliability in HVDC macrogrid, particular transmission paths in the WECC were suggested to be monitored, particular locations for HVDC connection points were suggested, use of HVDC in point-to-point of network configurations, there was also interest in having HVDC models open.
- In addition to the technical aspects of this project, IAB members showed interest in financial, market/business model, and cost/benefit of an HVDC macrogrid.
- Regarding regulatory framework for HVDC macrogrid, IAB members showed interest in: transmission charges, market coordination, and policy to harmonize market optimization reliability criteria when lines cross several market footprints, impact to existing seams coordination agreements and the ISO/RTO Council's congestion management process, and how generators would be paid for frequency response exported to other interconnections.

## 4.6 Presentations and publications

The following presentations and publications were produced:

- Journal paper manuscript submitted to CSEE Journal of Power and Energy Systems: M. A. Elizondo, N. Mohan, J. O'Brien, Q. Huang, D. Orser, W. Hess, W. Zhu, D. Chandrashekhara, Y. V. Makarov, D. Osborn, J. Feltes, H. Kirkham, D. Duebner, and Z. Huang, "HVDC Macro Grid Modeling for Power-flow and Transient Stability Studies in North American Continental-Level Interconnections," CSEE Journal of Power and Energy Systems, 2017.
- Suman Debnath, "Asynchronous Interconnects with Multi-Terminal VSC-HVDC", accepted in EPRI-HVDC conference.
- Suman Debnath, "MMC-HVDC low-inertia weak grid", accepted in IEEE PEDS conference
- Panel session presentation at IEEE PES General Meeting 2017 held in Chicago: Nihal Mohan (MISO) presented in Panel Session: Challenge in Operation and Control of AC-DC Hybrid Power Systems. Presentation title was "Multi Objective Control Strategies for HVDC Converters for Congestion Management and Frequency Response Services"
- Poster presentation at the GMLC project review in Washington DC, on April 18, 2017
- Presentations to industry advisory board:
  - June, 2017: teleconference presentation of main results of the project
  - December, 2016: teleconference presentation of use cases and scenarios of study
  - September, 2016: teleconference presentation on project description, and discussion of objectives and technical approach



## 5.0 References

- [ABB 2012] “HVDC and HVDC Light.” Montreal, Canada. Available <http://www.abb.com/hvdc> Accessed 11/26/2012.
- [Alstom Grid 2010] Multi-terminal HVDC System for Large Offshore Wind Park Grid Integration, Alstom Grid, Summer 2010. Pp. 24-26.
- [Arrillaga 2007] Arrillaga, J., Y.H. Liu, and N.R. Watson. 2007. Flexible Power Transmission. The HVDC Options, J. Wiley and Sons Ltd, Hoboken, NJ.
- [Asplund 2007] Asplund, G. 2007. “Ultra high voltage transmission.” ABB Review 2/2007, pp. 22-27. Available [http://www05.abb.com/global/scot/scot271.nsf/veritydisplay/9e16e26d65ab7339c12572fe004deb21/\\$file/22-27%20m733\\_eng72dpi.pdf](http://www05.abb.com/global/scot/scot271.nsf/veritydisplay/9e16e26d65ab7339c12572fe004deb21/$file/22-27%20m733_eng72dpi.pdf). Accessed 11/20/2012.
- [BAL-003-1 2008] Standard BAL-003-1 — Frequency Response and Frequency Bias Setting, 2008
- [Cigre 2008] TB 364 2008 WG B4.41 Systems with multiple DC Infeed
- [Debnath 2015] S. Debnath, J. Qin, B. Bahrani, M. Saedifard, and P. Barbosa, “Operation, control, and applications of the modular multilevel converter: A review,” *IEEE Trans. Power Electron.*, vol. 30, no. 1, pp. 37–53, Jan 2015.
- [Dommel 1969] H. W. Dommel, “Digital Computer Solution of Electromagnetic Transients in Single and Multiphase Networks”, *IEEE Trans. on Power Apparatus and Systems*, PAS-88, no. 4, pp. 388-399, April 1969.
- [Fairley 2016] P. Fairley, “Why Southern China Broke Up Its Power Grid,” *IEEE Spectrum*, December 2016
- [Huang 2002] Huang, H., V. Ramaswami, and D. Kumar. 2002. “Design Considerations of Ultra High Voltage DC System.” December 2002. Available [http://www.ptd.siemens.de/050714\\_Design\\_Considerations\\_UHVDC.pdf](http://www.ptd.siemens.de/050714_Design_Considerations_UHVDC.pdf). Accessed 10/31/2012.
- [Gnanarathna 2011] U. Gnanarathna, A. Gole, and R. Jayasinghe, “Efficient modeling of modular multilevel hvdc converters (MMC) on electromagnetic transient simulation programs,” *IEEE Trans. Power Del.*, vol. 26, no. 1, pp. 316–324, Jan 2011.
- [Golestan 2017] S. Golestan, J. M. Guerrero, and J. C. Vasquez, “Three-Phase PLLs: A Review of Recent Advances”, *IEEE Trans. Power Electron.*, vol. 32, no. 3, pp. 1894-1907, March 2017.
- [Green Economy 2011] “First HVDC Transmission Projects Beginning Globally.” *Green Economy*, May 2, 2011. Available <http://uk.ibtimes.com/articles/20110502/first-hvdc-transmission-projects-beginning-globally.htm>. Accessed 11/15/2012.
- [Gustavsen 1999] B. Gustavsen, G. Irwin, R. Mangelrød, D. Brandt, K. Kent, “Transmission Line Models for the Simulation of Interaction Phenomena between Parallel AC and DC Overhead Lines”, *IPST '99 Proceedings*, pp. 61-67, 1999.
- [Kirkham 2014] H. Kirkham, M Elizondo, and J Dagle. An Introduction to High Voltage dc Networks. Richland: PNNL, 2014.
- [Kou 2014] Gefei Kou et al., “Dynamic Model Validation with Governor Deadband on the Eastern Interconnection”, April 2014.
- [Kou 2016] G. Kou, P. Markham, S. Hadley, T. King, and Y. Liu, “Impact of Governor Deadband on Frequency Response of the U.S. Eastern Interconnection”, *IEEE Trans. on Smart Grid*, vol. 7, no. 3, pp. 1368-1377, May 2016.
- [Larruskain 2007] Larruskain, D.M., I. Zamora, O. Abarrategui, A. Iraolagoitia, M. D. Gutiérrez, E. Loroño, and F. de la Bodega. 2007. “Power Transmission Capacity Upgrade of Overhead Lines.” Department of Electrical Engineering, E.U.I.T.I., University of the Basque Country, Available [http://www.icrepq.com/icrepq06/296\\_Larruskain.pdf](http://www.icrepq.com/icrepq06/296_Larruskain.pdf). Accessed 11/20/2012.

- [Lescale 2008] Lescale, V.F., A. Kumar, L.-E. Juhlin, H. Björklund, and K. Nyberg. 2008. "Challenges with Multi-Terminal UHVDC Transmissions." POWERCON 2008 & 2008 IEEE Power India Conference, New Delhi, India, October 12-15, 2008. Institute of Electrical and Electronics Engineers, Piscataway, NJ.
- [Li 2015] Y. Li, and J.D. McCalley. "Design of a High Capacity Inter-Regional Transmission Overlay for the U.S." *IEEE Transactions on Power Systems*, vol. 30, no. 1, pp. 513-521, Jan. 2015.
- [Liu 2015] Z. Liu, et al., "Survey of technologies of line commutated converter based high voltage direct current transmission in China," *CSEE Journal of Power and Energy Systems*, 2015. 1(2): p. 1-8.
- [Makarov 2013a] Y.V. Makarov, M. Hunsaker, A. Diaz-Gonzalez, R. T. Guttromson, P. Du, P.V. Etingov, H. Ghoudjehbaklou, J. Ma, D. Tovar, V.V. Viswanathan, B. Vyakaranam, "WECC Variable Generation Planning Reference Book: A Guidebook for Including Variable Generation in the Planning Process," Volume 1: Main Document, Version 1, May 14, 2013. [Online.] Available: [https://www.wecc.biz/\\_layouts/15/WopiFrame.aspx?sourcedoc=/Reliability/WECC\\_Visible\\_Generation\\_Planning\\_Reference\\_Book\\_Main.docx&action=default&DefaultItemOpen=1](https://www.wecc.biz/_layouts/15/WopiFrame.aspx?sourcedoc=/Reliability/WECC_Visible_Generation_Planning_Reference_Book_Main.docx&action=default&DefaultItemOpen=1)
- [Makarov 2013b] Y.V. Makarov, M. Hunsaker, A. Diaz-Gonzalez, R. T. Guttromson, P. Du, P.V. Etingov, H. Ghoudjehbaklou, J. Ma, D. Tovar, V.V. Viswanathan, B. Vyakaranam, "WECC Variable Generation Planning Reference Book: A Guidebook for Including Variable Generation in the Planning Process," Volume 2: Appendices, Version 1, May 14, 2013. [Online.] Available: [https://www.wecc.biz/\\_layouts/15/WopiFrame.aspx?sourcedoc=/Reliability/WECC\\_Visible\\_Generation\\_Planning\\_Reference\\_Book\\_Appendices.docx&action=default&DefaultItemOpen=1](https://www.wecc.biz/_layouts/15/WopiFrame.aspx?sourcedoc=/Reliability/WECC_Visible_Generation_Planning_Reference_Book_Appendices.docx&action=default&DefaultItemOpen=1)
- [McDonald 2016] A. E. MacDonald, C.T. M. Clack, A. Alexander, A. Dunbar, J. Wilczak, and Y. Xie. "Future cost-competitive electricity systems and their impact on US CO2 emissions." *Nature Climate Change*, January 2016: 1758-6798.
- [MISO 2014] MISO Transmission Expansion Planning (MTEP) report. MISO, 2014
- [Morched 1999] A. Morched, B. Gustavsen, and M. Tartibi, "A Universal Model for Accurate Calculation of Electromagnetic Transients on Overhead Lines and Underground Cables", *IEEE Trans. on Power Del.*, vol. 14, no. 3, pp. 1032-1038, July 1999.
- [Mukhedkar 2011] Radnya Mukhedkar, "Introduction to HVDC: LCC & VSC – Comparison", Alstom, 2011
- [NERC 2011] NERC Resources Subcommittee, "Balancing and Frequency Control", pp. 1-53, January 2011.
- [NREL 2017] Project "Midwest Interconnection Seams Study," Grid Modernization Laboratory Consortium, U.S. Department of Energy, Washington, D.C. 2017
- [Perri 2017] E. Pierri, et al., "Challenges and opportunities for a European HVDC grid," *Renewable and Sustainable Energy Reviews*, vol. 70: p. 427-456. 2017.
- [Qingrui 2011] Qingrui Tu, Zheng Xu, and Lie Xu, "Reduced Switching-Frequency Modulation and Circulating Current Suppression for Modular Multilevel Converters", *IEEE Trans. Power Del.*, vol. 26, no. 3, pp. 2009-2017, July 2011.
- [Rao 2015] H. Rao, "Architecture of Nan'ao multi-terminal VSC-HVDC system and its multi-functional control," *CSEE Journal of Power and Energy Systems*, vol.1, no. 1 p. 9-18, 2015.
- [Saad 2014] H. Saad, S. Denetiere, J. Mahseredjian, P. Delarue, X. Guillaud, J. Peralta, and S. Nguefeu, "Modular multilevel converter models for electromagnetic transients," *IEEE Trans. Power Del.*, vol. 29, no. 3, pp. 1481–1489, June 2014.

- [Sellick 2012] R L Sellick, and M Akerberg, "Comparison of HVDC Light (VSC) and HVDC Classic (LCC) Site Aspects, for a 500 MW 400 kV HVDC Transmission Scheme", IET ACDC, Dec 2012.
- [Siemens PTI 2013] Siemens PTI, PSS®E Program User Manual, October 2013
- [Xia 2017] T. Xia et al., "Wide-area Frequency Based Event Location Estimation," 2007 IEEE Power Engineering Society General Meeting, Tampa, FL, 2007, pp. 1-7.
- [Xu 2017] C. Xu, A New Energy Network: HVDC Development in China. 2017; Available from: <http://cleanandsecuregrid.org/2017/01/02/a-new-energy-network-hvdc-development-in-china/>
- [Zhang 2004] Zhang, X.-P. 2004. "Multiterminal voltage-sourced converter-based HVDC models for power flow analysis." IEEE Transactions on Power Systems, vol. 19, no. 4, Nov., pp. 1877-1884.
- [Zhou 2016] H. Zhou, Y. Su, Y. Chen, Q. Ma and W. Mo, "The China Southern Power Grid: Solutions to Operation Risks and Planning Challenges," in IEEE Power and Energy Magazine, vol. 14, no. 4, pp. 72-78, July-Aug. 2016.



## **Appendix A**

### **Advanced HVDC dynamic modeling**



## A.1 MMC-HVDC DAEs

From Figure 12, the arm currents' dynamics are given by

$$\begin{aligned}
(L_o + L_s) \frac{di_{p,j}}{dt} - L_s \frac{di_{n,j}}{dt} &= -(R_o + R_s) i_{p,j} + R_s i_{n,j} + \frac{V_{dc}}{2} - v_j - v_{cm} - v_{p,j}, \forall j \in (a, b, c), \\
(L_o + L_s) \frac{di_{n,j}}{dt} - L_s \frac{di_{p,j}}{dt} &= -(R_o + R_s) i_{n,j} + R_s i_{p,j} + \frac{V_{dc}}{2} + v_j + v_{cm} - v_{n,j}, \forall j \in (a, b, c), \\
v_{y,j} &= \sum_{i=1}^N v_{sm,y,i,j} = \sum_{i=1}^N [S_{yi1,j} v_{cy,i,j} + \{(1 - S_{yi1,j})(1 - S_{yi2,j}) v_{cy,i,j}\} \operatorname{sgn}(i_{y,j})], \forall y \in (p, n), \forall j \in (a, b, c), \\
\operatorname{sgn}(x) &= \begin{cases} 0 & \text{if } x < 0 \\ 1 & \text{if } x > 0, \end{cases} \quad v_{cm} = \frac{1}{6} \sum_{j=a,b,c} (v_{n,j} - v_{p,j}), \quad \sum_{j=a,b,c} i_{p,j} = \sum_{j=a,b,c} i_{n,j}
\end{aligned} \tag{A.1.1}$$

The capacitor voltages' dynamics are given by

$$C_{SM} \frac{dv_{cy,i,j}}{dt} = -\frac{v_{cy,i,j}}{R_p} + S_{yi1,j} i_{y,j} + (1 - S_{yi1,j})(1 - S_{yi2,j}) i_{y,j} \operatorname{sgn}(i_{y,j}), \forall y \in (p, n), \forall j \in (a, b, c). \tag{A.1.2}$$

Equations (A.1.1) and (A.1.2) represent a semi-explicit DAE with numerical stiffness introduced because of the presence of  $\operatorname{sgn}$  function. The  $\operatorname{sgn}$  function arises from the modeling of diodes that are present in the MMC-HVDC. The  $\operatorname{sgn}$  function introduces numerical stiffness in the arm currents' dynamics. The numerical stiffness is observed only in the arm currents' dynamics as the  $\operatorname{sgn}$  function in the capacitor voltages' dynamics can be treated as an external input.

In normal operating conditions, one of the switches in the half-bridge SM is in ON-state. If the upper switch is in ON-state, the SM is said to be in ON-state. If the lower switch is in ON-state, the SM is said to be in OFF-state. When the SM is in ON/OFF state, the  $\operatorname{sgn}$  functions in (A.1.1) and (A.1.2) are no longer present and the dynamics of the arm currents and capacitor voltages can be deduced to

$$M_1 \frac{dx_1}{dt} = Ax_1 + Bs + Cz, \tag{A.1.3}$$

where the variables are defined by

$$\begin{aligned}
M_1 &= \begin{pmatrix} L_o + L_s & -L_s & 0 & 0 & 0 \\ -L_s & L_o + L_s & 0 & 0 & 0 \\ 0 & 0 & L_o + L_s & -L_s & 0 \\ 0 & 0 & -L_s & L_o + L_s & 0 \\ -L_s & L_s & -L_s & L_s & L_o \end{pmatrix}, \\
A &= - \begin{pmatrix} R_o + R_s & -R_s & 0 & 0 & 0 \\ -R_s & R_o + R_s & 0 & 0 & 0 \\ 0 & 0 & R_o + R_s & -R_s & 0 \\ 0 & 0 & -R_s & R_o + R_s & 0 \\ -R_s & R_s & -R_s & R_s & R_o \end{pmatrix}, \\
B &= \begin{pmatrix} 0.5 & -1 & 0 & 0 \\ 0.5 & 1 & 0 & 0 \\ 0.5 & 0 & -1 & 0 \\ 0.5 & 0 & 1 & 0 \\ 0.5 & 0 & 0 & -1 \end{pmatrix}, \\
C &= \begin{pmatrix} -5/6 & -1/6 & 1/6 & -1/6 & 1/6 & -1/6 \\ -1/6 & -5/6 & -1/6 & 1/6 & -1/6 & 1/6 \\ 1/6 & -1/6 & -5/6 & -1/6 & 1/6 & -1/6 \\ -1/6 & 1/6 & -1/6 & -5/6 & -1/6 & 1/6 \\ 1/6 & -1/6 & 1/6 & -1/6 & -5/6 & -1/6 \end{pmatrix}, \\
s &= (V_{dc} \quad v_a \quad v_b \quad v_c)^T, \\
x_1 &= (i_{p,a} \quad i_{n,a} \quad i_{p,b} \quad i_{n,b} \quad i_{p,c})^T, \\
z &= (v_{p,a} \quad v_{n,a} \quad v_{p,b} \quad v_{n,b} \quad v_{p,c} \quad v_{n,c})^T.
\end{aligned}$$

Equation (A.1.3) represents a linear ordinary differential equation (ODE) if  $z$  can be treated as an input variable. There is no  $\text{sgn}$  function present under these conditions and hence, there is no numerical stiffness associated with the arm currents' dynamics.

In blocked condition, both the switches in the half-bridge SM are in OFF-state. The blocked condition arises during external faults. Under this condition, the  $\text{sgn}$  function present in (A.1.1) introduces numerical stiffness in the arm currents' dynamics.

## A.2 Multi-terminal VSC-HVDC control approach

### A.2.1 Inner-loop control system

The internal control system comprises  $qd$  AC-side current control and  $qd$  circulating current control of the second- and fourth-order harmonics. The AC-side current and circulating current control strategies are based on the strategies described in [Qingrui 2011]. Control of fourth-order harmonic in the circulating current is not considered in [Qingrui 2011]. The control of fourth-order assumes significance if a third harmonic is injected in the modulation indices. The presence of third harmonic improves the range of modulation indices, but introduces a fourth harmonic component in the circulating current.

In addition to the  $qd$  AC-side and circulating currents' control,  $\theta$ -component of the circulating current and the average of all the submodule (SM) capacitor voltages in the MMC (defined by  $v_c^\Sigma$ ) are controlled for better dynamic performance and for greater flexibility. The reference for  $v_c^\Sigma$ ,  $v_{c,\text{ref}}$ , is varied based on the operating conditions so as to avoid saturation of the arm modulation indices. The summary of internal control system is shown in Figure 44.

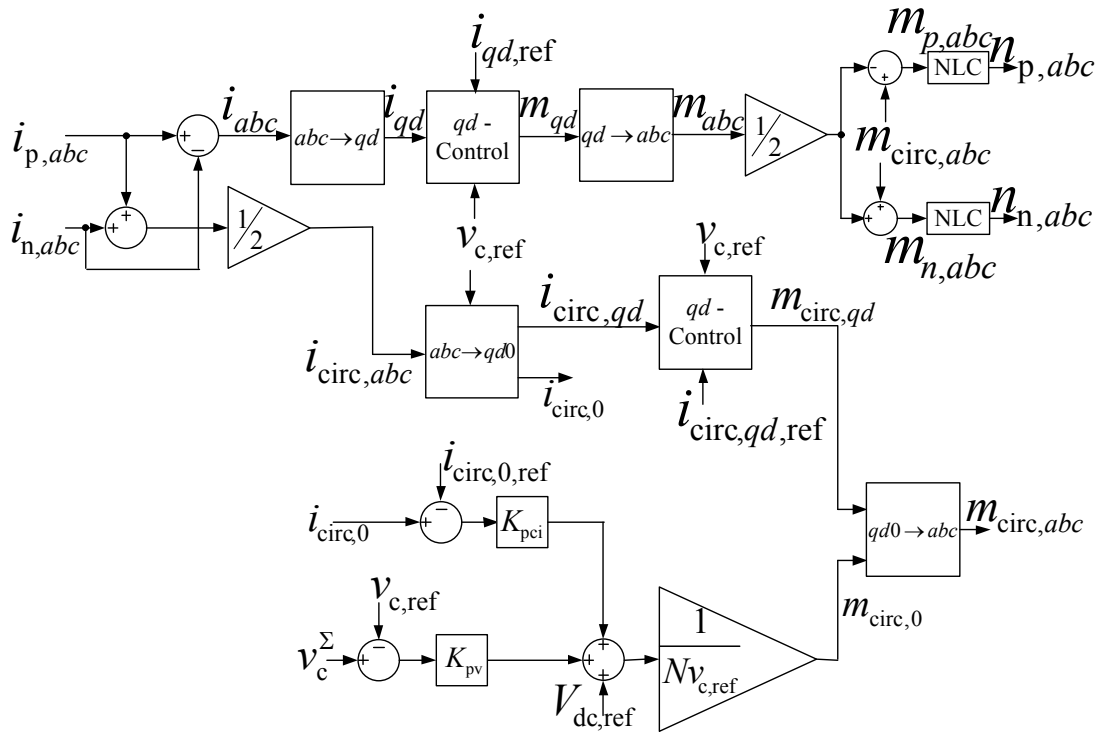


Figure 44: Summary of internal control system

### A.2.2 SM capacitor voltage balancing algorithm

The voltage balancing strategy of the SM capacitors in an MMC is shown in Figure 45. The algorithm is based on minimizing the switching frequency of the SMs, while constraints are imposed on the maximum SM capacitor voltage. While the reduction in switching frequency improves the efficiency of operation, the constraints on the maximum SM capacitor voltage ensures that the semiconductor devices do not operate beyond their rated operating voltages.

The algorithm is based on turning ON/OFF the SMs, at any instant, with maximum/minimum capacitor voltages based on the direction of the corresponding arm current. For instance, if the arm current is positive and a certain number of SMs need to be turned ON (named as delta in the figure), the SMs with the minimum capacitor voltages amongst the OFF-state SMs are turned ON. A positive arm current indicates that the current is charging the SM capacitors.

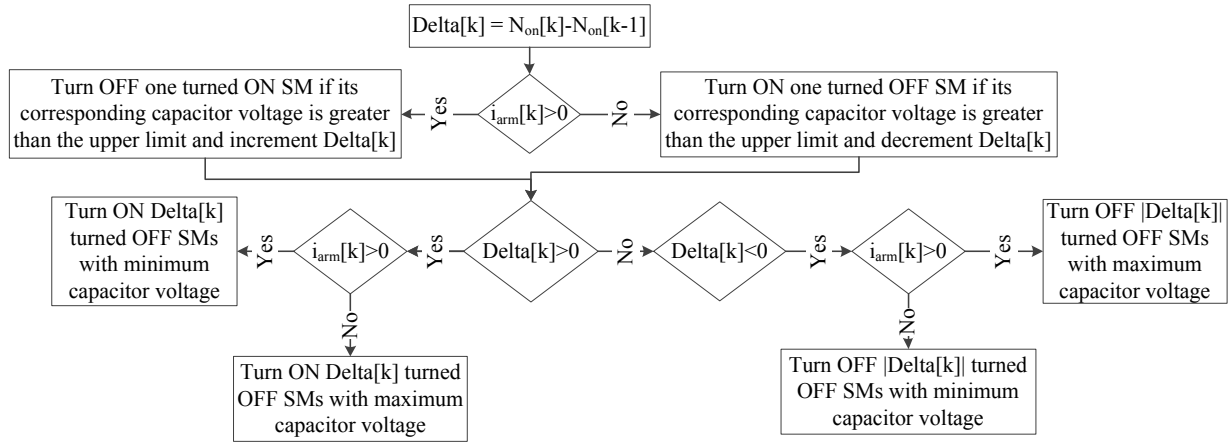


Figure 45: MMC submodule capacitor voltage balancing algorithm.





---

Address Line 1  
Address Line 2  
City, ST Zip  
Phone Number

<http://gridmodernization.labworks.org/>